Aus dem Zentrum für Unfallchirurgie und Orthopädie (ZOU)

der Universitätsmedizin der Johannes-Gutenberg-Universität Mainz

The influence of different antiadhesive polymer coatings on the adhesion and proliferation of fibroblasts and tenocytes

Einflüsse verschiedener antiadhäsiver Polymerbeschichtungen auf die Adhäsion und Proliferation von Fibroblasten und Tenozyten

Inauguraldissertation

zur Erlangung des Doktorgrades der Medizin

der Universitätsmedizin

der Johannes Gutenberg-Universität Mainz

Vorgelegt von

Kira Vogel

aus Unna

Mainz, 2025

Wissenschaftlicher Vorstand: Univ.-Prof. Dr. Philipp Drees

1.Gutachter:

2. Gutachter:

Tag der Promotion: 09.02.2026

Contents

Abbreviations

°C	degree Celsius
AD	adhesion polymer
approx.	approximately
BSA	bovine serum albumin
CFU	colony forming units
CNN1	Calponin 1
CT	threshold cycle
D	day
DMSO	Dimethylsulfoxid
e.g.	exempli gratia
ECM	extracellular matrix
eGFP	enhanced green fluorescent protein
etc.	et cetera
FACS	Fluorescence-activated cell sorting
FBSS	Failed- back surgery syndrome
FC	fully coated
FCS	Fetal Calf Serum
FR	free radical polymerization
h	hora (hour)
HAI	hospital-acquired infection
HRQoL	Health-related Quality of Life
CDC	Centre of Disease Control
MHA	Müller Hinton Agar
MTT	3-(4,5-dimethylthiazol-2-yl) -2,5-diphenyltetrazolium bromide
NHDF	normal human dermal fibroblasts
PBS	phosphate buffered saline
PC	partially coated
PCR	polymerase chain reaction
PFA	paraformaldehyde
POA	post-operative Adhesions
rpm	revolutions per minute
SSI	surgical site infection

TNDM	Tenomodulin
vWF	van Willebrand factor

List of Figures:

List of Charts

1 Zusammenfassung – deutsche Version

Die Behandlung von Frakturen mittels Implantaten ist ein großes Gebiet innerhalb der Unfallchirurgie und der orthopädischen Chirurgie. Wenn das Implantat keine Probleme bereitet, muss nicht unbedingt eine Materialentfernung erfolgen und das Implantat verbleibt im Körper. Es gibt jedoch durchaus Indikationen zur Materialentfernung, allen voran die Infektion. Jedoch auch gelenknahe Implantate können, und jene welche bei der Mobilisation hinderlich sind, sollten entfernt werden. Im Vordergrund steht hier auch der Wunsch des Patienten nach einer Implantatentfernung. Gerade in Bereichen in denen Sehnen beteiligt sind oder nah an der Osteosynthese liegen wie z.B. bei palmaren Platten bei distalen Radiusfrakturen, sind Komplikationen wie Arrosionen der Sehnen nach Implantatentfernung beschrieben. (2) Diese Prozeduren machen einen Großteil der orthopädisch/unfallchirurgischen Eingriffe aus (30.5% im Jahr 2020 in Deutschland (3)) und gehen mit nicht unerheblichen Risiken einher, wie persistierenden Schmerzen und Refrakturen. (4)

Diesem zugrundeliegenden klinischen Problem haben wir uns gewidmet und haben Polymerbeschichtungen auf ihre antiadhäsiven Eigenschaften hin getestet. Auf die Beschichtungen wurden in vitro humane Fibroblasten und selbstisolierte Tenozyten ausgesät, welche aus Spendermaterial gewonnen wurden. Diese wurden immunhistochemisch und mittels RT-PCR weiter auf ihre spezifischen Eigenschaften und Marker getestet. Um die Zellen auf den Beschichtungen sichtbar zu machen, wurden diese mittels eines lentiviralen Vektorsystems mit grün fluoreszierendem Protein transduziert. Des Weiteren wurden zwei Polymerbeschichtungen getestet bei denen **N** eine klare antibakterielle Eigenschaft gegen Staphylococcus aureus gezeigt hat. Außerdem wurden die Beschichtungen auf ihre zytotoxischen Eigenschaften hin mittels MTT-Assay getestet. Hierbei waren einige Beschichtungen klar als zytotoxisch zu bewerten andere jedoch zeigten eine gute Biokompatibilität und wurden als vielversprechend eingestuft. Im Großen und Ganzen haben sich zwei Beschichtungen, **A** und **N** für die weiteren Versuche auf Titanplatten und ggf. Im folgendem im Kleintiermodell qualifiziert, da insbesondere **N** zusätzlich antibakterielle Eigenschaften besitzt und beide Beschichtungen jeweils für Fibroblasten und Tenozyten sehr gute antiadhäsive Eigenschaften gezeigt haben sowie biokompatibel sind.

Insgesamt jedoch sollte man hierbei jederzeit bedenken, dass die gewonnenen Erkenntnisse dadurch eingeschränkt sind, da sie in vitro gewonnen wurden und nur

eine sehr beschränkte Aussage zur Übertragbarkeit der Effekte in vivo getroffen werden kann.

Es handelt sich hierbei jedoch um einen äußerst vielversprechenden und neuartigen Ansatz in der Entwicklung von anti-adhäsiven und zudem gleichzeitig antibakteriell wirkenden Beschichtungen für Kurzzeitimplantate, die in weiteren Untersuchungen für den Gebrauch in vivo getestet werden sollten, um implantatassoziierte Komplikationen in der Zukunft zu reduzieren.

2 Introduction

Post-operative complications after the surgical repair of fractures in the small bones can resolve in a serious impact to the patient. Scarring of tissue can lead to immobilization which can be fatal for further function. Common complications of fracture repair called osteosynthesis can often be put down to adhesion of soft tissue on implants as well as surgical site infections. Particularly, when small, temporary implants are used (for example in hand and foot surgery), complications of soft tissue and tendon adhesions can be severe regarding the function of small joints. (5) Because of the development of scar tissue, the involved cell types of this process mainly include fibroblasts and tenocytes as the tendons are in proximity to the used implants.

As these implants are meant to be removed after a certain period, the formation of adhesions at the surgical site can cause complications with removal as cell adhesion is a widespread complication in modern medicine. Surface modifications of different short-term implants like osteosynthesis material as well as e.g. catheters is a way to reduce these complications. Especially the impairment of tendons after osteosynthesis or after tendon injury can result in a heavy socioeconomic burden and reduced quality of life. The follow-up treatment and recovery from tendon injuries is prolonged and results in a median of 50 days of illness per injury, which leads to a major challenge in clinical management. (6)

Therefore, the aim to create a barrier against adhesion and infection is an area of interest for numerous research teams. Antibacterial coatings, polymer hydrogels and different surface modifications are only some of them. It is important to note that these surface modifications must resist against cell adhesion without creating a cytotoxic environment to the surrounding tissue.

All in all, we faced a problem that is a socioeconomic burden on the one hand and a serious medical issue on the other hand as it can significantly increase postoperative as well as intraoperative complications with implant removal or impairment of motion.

2.1 The aim of this scientific study

The aim of this scientific study was to characterize different polymers to highlight those with the best anti-adhesive and antibacterial qualities without being cytotoxic to their surrounding tissue.

We observed the characteristics of different polymer coatings in contact with cell lines of the human body to see if they showed potential to act as a barrier against cell adhesion. The polymers varied for example in their side chains which resulted in different anti-adhesive features. Tenocytes were isolated from human donor material and further characterized with immunofluorescence and PCR.

In this part of our work, the polymers were tested in vitro as the coatings were seeded on well-plates and tested with fibroblasts and tenocytes, made visible with green fluorescent protein inserted into the cell's genome via a lentiviral vector. Photography was taken at regular intervals to control the growth on coated as well on non-coated areas. As it is very important that the coatings acted against cell adhesion but were non-cytotoxic themselves, they were tested with the MTT Assay (a cell viability assay) to rule out coatings with cytotoxic characteristics. Additionally, a cell culture was set up with the cells which had been in contact with the coatings to observe their growth potential. Again, photography was taken. Furthermore, two polymers were tested on their antibacterial properties.

3 Literature review

3.1 Osteosynthesis and Fracture healing

Fractures show a high lifetime prevalence with 44% in adults aged 55 or older. (7) Especially in the older population, the incidence of fractures is expected to rise due to higher life expectancy. (8) In their detailed analysis of, Rupp et al. stated the recording of 688.403 fractures in 2019 in Germany which shows an increase of 14% compared to 2009. The most common were femoral neck fractures (120 per 100.000 persons per year), pertrochanteric femoral fractures (109 per 100.000 persons per year) and the fractures of the distal radius (106 per 100.000 persons per year). (9)

Osteosynthesis:

Depending on the type of fracture and/or the patients claim to physical activity, injuries to the bone are either treated conservatively or surgically. Surgical treatment of bone injury includes several methods of internal or external fixation after reduction of the fracture. A well-established process for fracture treatment is plate osteosynthesis (see figure 1). The injured bone is realigned to its anatomical form and is temporarily fixated with reduction forceps. After controlling the reposition, the plate is selected and formed to fit the bone. Then, screws are inserted to hold the plate in place and to reach internal fixation (e.g. with angle-stable plates, where there is a screw thread in each hole to ensure stable fixation of fragments).

Figure 1: Plate osteosynthesis for a diaphyseal metacarpal (hand bone) V fracture. Picture taken from Siemers, F. : Konservative und operative Therapie von Mittelhandfrakturen (10)

Other methods for fracture treatment include intramedullary nailing systems, tension band plating or external fixator systems in acute trauma management.

Fracture healing:

Bone healing is a complex physiological process involving a lot of steps to regenerate bone tissue after trauma (fracture).

Fracture healing can be subdivided into two groups:

- **primary fracture healing**
- **secondary fracture healing**

The main goal is to restore the bones mechanical stability and vascular supply via angiogenesis and defect compensation. (11)

Primary fracture healing:

The reparation process which leads to primary fracture healing is characterized by direct bone repair lacking endochondral ossification. A crucial requirement for this is an optimal surgical reduction of fracture ends. (11, 12)

As of this, direct or primary fracture healing is not that common. If all requirements are met, primary healing occurs by direct remodeling of blood vessels, Haversian canals and lamellar bone. The process of primary healing takes months to a few years until fully done. Primary healing happens via contact healing or gap healing:

- Contact healing:

Contact healing occurs if the interfragmentary gap is less than 0.01mm and the strain less than 2%. So called cutting cones which are formed by osteoclasts can cross the fracture line hereby creating cavities which are filled up by osteoblasts. In this way, new Haversian systems are created along with bone union. This process results in lamellar bone without callus formation.

- Gap healing:

The difference to contact healing is that bone union and the Haversian remodeling do not occur simultaneously. Fracture gap needs to be less than 800µm to 1mm. Here, the fracture is perpendicularly filled with lamellar bone which must undergo secondary

remodeling. Over the course of three to eight weeks, cutting cones and longitudinal osteons are developing. The restore the anatomical and biomechanical integrity of the bone. (13)

Secondary fracture healing:

If the ends of the fracture don't match or if there is a major defect zone, primary healing does not occur. The bone must build callus to overcome the fracture gap. Three overlapping stages are observed in secondary healing. An initial inflammatory response, callus formation (subdivided in soft and hard callus) as well as initial bony union and bone remodeling. (12)

In the inflammatory phase, local chondrocytes in the fracture site hematoma get hypertrophic, mineralize and are exchanged through osteocytes. At first, soft callus and later hard callus is created. (14)

The following chart gives an overview on the different phases and bone formation processes in secondary fracture healing.

Phase	Time span	Process
inflammatory	first week	formation of fracture site hematoma
soft callus formation	second until third week	formation of granulation tissue
hard callus formation	< three to four months	storage of Ca^{2+} woven bone formation
remodeling	years	lamellar bone formation remodeling processes by osteoblast and osteoclasts adapting to biomechanical needs

Chart 1: Phases of secondary fracture healing. Modified from Badia et. al (12)

3.2 Surgical Site Infection

An infection of osteosynthesis which is called surgical site infection (SSI) can resolve in major problems for the patient. SSI's take up a numerous number of hospital-acquired infections (HAI). In Europe during the years 2011-2012, the proportion of surgical site infections was 19.6%. (15)

A SSI was defined by the Centre for Disease Control and Prevention (CDC) as a postoperative infection which occurs 30 days after a surgical intervention, involves the subcutaneous tissue and either pus draining from the incision, evidence of organisms in normally aseptic environment, signs and symptoms of infections and the diagnosis of a SSI by the surgeon. (16)

Infections of implants in osteosynthesis is mainly caused by Staphylococcus aureus or gram-negative bacilli. (17) Risk factors for SSI's can be classified to **patient-related factors** (e.g. diabetes mellitus, high age, immunosuppression, smoking etc.), **wound factors** (grade of contamination of a wound: aseptic with a risk of infection <2%, conditionally aseptic with a risk <10%, contaminated with a risk of 5-20 % and septic with a risk of >20%) and **operative/ intervention specific factors** (localization like the axilla, perineum or groin, duration of the operation of hypothermia as well as hypoxia). (18-21)

The socioeconomic burden and increase of healthcare costs as well as the increased morbidity and mortality due to SSI's was studied by Badia et al. in a systematic review in six European countries. They found that for Germany, the total medial cost per patient was highly elevated (€36.261 vs €13.356). The data indicated that the intensive care unit and ward-care costs accounted for the highest amount of costs (27.7% and 24.7%). In cardiothoracic surgery, the length of stay was prolonged following a SSI (17.9 days), also mortality rate was double in patients with SSI's. Studies in the UK also showed significant reduction in Quality of Life, date acquired with Health-related Quality of Life Scores (HRQoL) indicate 11% reduction at 30 days in patients after laparotomy compared with those who did not develop a SSI. (15)

Treatment of SSI's involves incision and irrigation of the wound to drain a possible abscess formation, the surgical debridement of necrotic tissue and daily wound care. Superficial SSI's do not necessarily require systemic antibiotics. In septic or

immunocompromised patients, empiric antibiotic therapy is indicated, and de-escalation is performed when the antibiogram is at hand. (22)

As important as the treatment for SSI is the prevention of infection on the first hand. Risk factors were identified and should be minimized as much as possible to prevent postoperative infections. These included basic hygiene precautions like the proper reprocessing of medical devices, hand hygiene, disinfection of the operating field, avoidance of artificial nails and wearing jewelry. Also, patient-specific precautions like avoiding smoking, shorter preoperative hospital stay, screening for preexistent infections like (methicillin resistant staphylococcus aureus) MRSA and weight reduction were identified. (21)

Osteomyelitis:

The infection of the bone, known as osteomyelitis, also poses a significant clinical challenge to physicians. Different types of osteomyelitis exist, leading to different approaches in therapeutic strategies. One can see posttraumatic osteomyelitis due to an open wound/fracture, post-surgical osteomyelitis (e.g. after arthroplasty) or secondary osteomyelitis associated with poor vascularity or due to hematogenous infections. Where an acute osteomyelitis can sometimes be treated with antibiotics alone, chronic forms need to be treated in a multidisciplinary approach including systemic antibiotic treatment as well as surgical debridement. (23)

The onset of symptoms in posttraumatic and postoperative osteomyelitis marks an important part in subdividing the infection to acute (timespan of two weeks after surgery or trauma), subacute (two to six weeks) or chronic (over 6 weeks). (24)

As mentioned above, Staphylococcus aureus is considered as a main pathogen in implant-related infections, followed by Pseudomonas aeruginosa. (25) As Staph. aures is able to form a biofilm on implants, antibiotic treatment is getting more difficult. (23) Biofilms are formed by a microbial community in which cells attach to each other or an interface and are encased in an extracellular polymeric substance matrix experiencing changes in growth, protein production or phenotype. (26) These biofilms protect the pathogens in form of a diffusion barrier against antimicrobial substances. (23)

Clinical management of peri-implant infections:

Postoperative infection rate in Germany after osteosynthesis was described between 1.15% and 2.04% by the Robert-Koch-Institute for the years 2017-2019. (25)

Symptoms of acute osteomyelitis include the common signs of infection like erythema, pain, swelling or sometimes fever which can be totally absent in patients with chronic osteomyelitis. The diagnostic pathway includes clinical inspection of the wound, laboratory evaluation (elevated C-reactive protein, leukocytosis, positive blood cultures e.g.) and imaging (plain radiograph, magnet resonance imaging or bone scintigraphy). (27)

The most important, primary strategy is an antibiotic therapy in the management of an acute osteomyelitis. Calhoun et al. described that in some cases, when diagnosed early and treated with sensitive antibiotics, the cure rate for an acute osteomyelitis can reach up to 80%. (28, 29)

Obtaining microbial samples during operation is essential to further analyze and characterize the pathogen as well as testing of sensitive antibiotics. It is important to obtain at least three to six samples of representative areas without contamination. These samples are of a high value for further treatment options. (25)

When antibiotics alone are not sufficient, surgical therapy and/ or implant removal can be necessary. This includes radical debridement of the macroscopically infected and affected necrotic bone as well as soft tissue. Sometimes, when wounds are not found suitable for closure, vacuum assisted wound systems can be helpful. Implant removal can be considered with persisting infections after multiple debridement's. (30)

An early management of acute osteomyelitis is highly important for the outcome of the patient. Antibiotic therapy is crucial and needs to be adapted to the pathogen (mostly Staph. aureus) as well as obtaining microbial samples during surgery. Implant removal can be necessary if debridement alone is not sufficient. All in all, treatment and strategies need to be adapted to the underlying cause of osteomyelitis (acute or chronic) but can be very promising if treatment is started early.

3.3 Cell adhesion, clinical consequences and strategies of prevention

In orthopedic surgery, short-term implants like titanium plates for osteosynthesis or prostheses in knee or hip arthroplasty are used. While these short-term implants are frequently removed after fracture healing, an arthroplasty should last as long as possible with good osteointegration. (31) It is not uncommon that we are observing complications with implant removal, so it is in our interest to minimize the contact and/ or integration with the surrounding tissue to enable implant removal without major damage. With osteosynthesis materials like titanium plates, adhesion is an unrequired event as the surrounding tissue forms a scar, also affecting tendons, nerves and other structures. This can seriously affect the patient's mobility, in the worst case leading to periarthritis as well as a reduced quality of life. (32, 33)

Not only orthopedic surgery uses implants and foreign materials. Multiple applications of foreign body material exist in modern medicine. To apply drugs, a peripheral intravenous catheter is used, parenteral nutrition is applied via a gastric tube and to drain urine from the bladder, a flexible catheter is inserted. These are examples for mostly temporary implants which must be changed frequently to prevent infection and/ or cell adhesion. In contrast to those temporary implants, others need to stay for a longer period. In clinical practice, cell adhesion is undesired in all forms of foreign body material as well as bacterial colonization as it poses a threat of infection.

Post-operative Adhesions (POA) can be the result of a surgical procedure as well as trauma. (34) It is defined as hyperplasia of abnormal tissue that generates between organs. (35) A fibrinous network forms in the granular tissue which subsequently replaces necrotic tissue at the site of the damage (operation wound/ traumatic wound). This can cause fibrinous adhesion and lead to reduced function of the surrounding tissue. (32) This fibrinous tissue histologically consists of a mixture of cell types like eosinophils, fibroblasts, macrophages, mast cells and red blood cells. (36) Figure 2 gives a brief overview of the process of postoperative adhesion formation.

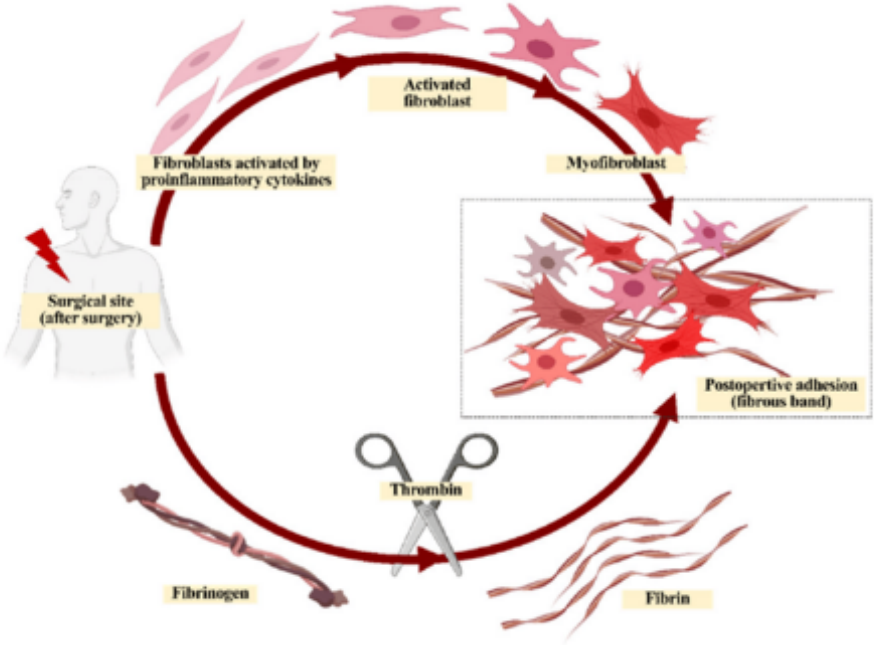

Figure 2: A simple schematic of the postoperative adhesion formation. Picture taken from Ishiyama et al. (1)

These adhesions can lead to multiple clinical consequences. They occur in various numbers of tissues leading to various, organ-specific problems for the patient. Most common POA's with a huge clinical impact are adhesions of the peritoneum, pericardium, tendons, intestinal adhesions, the dural sac and uterine adhesions. The variety of problems which can result from adhesions again highlights the clinical impact and need for anti-adhesive prevention strategies. (32)

The following chart illustrates the above-mentioned types of adhesion and their incidence as well as their relevance in clinical practice.

Type of POA	Occurrence	Incidence Rate	Clinical consequences
Tendon Adhesion	Tendon surgery	30-40% in patients 10% of recurrent adhesion	Mobility⇓ Periarthritis Articular dyskinesia
Peritoneal Adhesion	Abdominal and pelvic surgery	90% in patients 80% of recurrent adhesion	Intestinal Obstruction 65-75% of all small bowl obstructions, 32 % of acute intestinal obstructions pain Infertility in ♀
Pericardial Adhesion	Cardiothoracic surgery	6-17% of all valve repair and bypass surgeries	Higher risk of cardiac failure

	(e.g. bypass)		Increased risk of injury to heart, lung and greater vessels
Epidural Adhesion	Failed back surgery syndrome (FBSS)	8-40% of patients after laminectomy suffer from FBSS 24% of patients with FBSS develop an epidural scar	Back and leg pain Dural tears Injuries to the root of the nerve
Intrauterine Adhesion	Pregnancy, intrauterine device placement, Cesarean section, abortion and curettage	3.6 % in polyp removal 6.7% after resection of septa 21.6% after myomectomy, 37.6% after abortion curettage Risk for recurrent adhesion in moderate adhesion 23%, 62% for severe adhesion	Oligomenorrhea, amenorrhea, infertility Influence on physical and mental health

Chart 2: Types of post-operative adhesions with clinical consequences. Modified from Liao et al. (33)

Materials used for implants in orthopedic surgery include titanium or stainless steel. The implants must meet certain criteria as they need to deliver stability to ensure fracture healing. Implants need to have stiffness, strength, biocompatibility and ductility. Titanium and stainless steel differ in their mechanical properties as stainless steel is stiffer compared to titanium which approximately matches the elasticity of bone. (37) A difference regarding soft tissue adhesion could yet not be significantly proven. There exist few studies about tendon adhesion after osteosynthesis with titanium vs. stainless steel implants but animal studies of Sinicropi et al. indicated a higher amount of tendon inflammation with titanium implants than with stainless steel implants. They investigated 18 dogs and histologically analyzed the tendons after four months. (38) Yet others found no difference with dogs and rabbits. (37)

Adhesions of the tendon sometimes need to be corrected in another operative procedure called tenolysis. There are no strict indications to perform tenolysis as the patient's functional demands depend on many factors as occupational activity or age. If the patient's demands are high, a tenolysis or tenoarthrolysis where the joint and tendons are released from adhesions to improve mobility can be indicated. Clinical outcome cannot be foreseen as in some patients, limitations of the range of motion may persist or even worsen. (39, 40)

This indicates that the importance of prioritizing prevention of adhesions in the first place should be a therapeutic goal.

Current strategies of prevention:

Liao et al sorted the current strategies of preventing POA's by its way of occurrence:

Adhesion and deposition of fibrin and cells is met by strategies to construct an ideal surface e.g. with creating a rough surface, a dense porous surface or application of antifouling materials like poly-hydrophilic materials. Excessive deposition of fibrin hematoma or macrophage-fiber clot is met by anticoagulation agents to decrease fibrin formation, promoting the fibrinolytic system by fibrinolytic agents, promotion of hemostasis or inhibiting macrophage aggregation. Chronic inflammation is tried to be reduced by applying anti-inflammatory agents like dexamethasone, ibuprofen and others as well as establishing a negative-charged surface. The interconnection of tissue is tried to be reduced by physical barriers like hydrogels, electrospinning films or cast film. Abnormal rearranging of the extracellular matrix is met with inhibiting myofibroblast formation via chemical cues like TGF inhibitors or mechanical cues like hierarchical micro of nanoscaled scaffolds. Excessive vascularization is met with inhibiting fibroblast proliferation, inducing fibroblast apoptosis, vascular growth factor inhibitors like Bevacizumab or promoting the degradation of the extracellular matrix. (33)

In contrast to all those methods to reduce adhesion, in some types of implants like total hip arthroplasty, the adhesion or in this case osteointegration which describes the ingrowth of the implant into the bone is highly desired as a loose implant can lead to pain and therefore also a highly reduced quality of life. Implant-associated infections should be avoided at any cost, creating a demand for surface modifications of implants to promote osteointegration and reduce infections. This surface modifications include creating a certain roughness of the surface or different types of coatings like hydroxyapatite, metallic oxides or polymers. (41)

3.4 The use of polymers for adhesion prevention

Polymers are used for various purposes in modern medicine. There are polymers whose compounds can be found naturally which are called natural polymers. Hyaluronic acid, proteins, silk, fibrin and alginate are only a part of them. They have been used widely for tissue engineering, acting as drug delivery carriers or helping promote wound healing. On the other hand, polymers that are synthesized are called synthetic polymers, e.g. poly (lactic acid), poly (acrylic acid). Many of them have excellent biocompatible properties and are therefore the center of multiple studies. (42) Advantages of polymeric biomaterials in biomedical use are for example the numerous possibilities of modification and in general the low production costs. (43)

Synthetic and natural derived polymers both have their specific advantages and disadvantages. Naturally found polymers show extremely good biocompatibility and biodegradability, yet they are inferior in mechanical properties and have poorer output stability whereas synthetic polymers show more chemical stability and have a lot of potential for modification. Despite its benefits, their reduced biocompatibility can result in an increased inflammatory potential. (32)

As polymers can form bonds with a surface which result in an irreversible coating, they are often used in surface coating applications not least because of its high molecular weight and its chain length.(42)

An interesting aspect of preventing post-operative adhesions is the use of polymeric hydrogels. These can again be of natural as well as of a synthetic origin. By cross-linking, synthetic polymer hydrogels can be creating with e.g. polyethylene, polyacrylic acid and others. (32) For example, Ishiyma et al. (1) created a hydrogel consisting of polymethyl methacrylate and amphiphilic polybutyl methacrylate with Fe^{3+} ions. Interesting is, that these water-soluble polymers perform cross-linking in situ. The influence of this hydrogel on tendon adhesion and tendon healing in chickens and rats was observed. They found that the application of synthetic hydrogel polymer was able to prevent post-operative adhesion without negatively affecting the process of tendon healing.
The use of polymers (natural and synthetic) in adhesion prevention is already vast and gradually expanding and will be subject of many future studies.

3.5 Tendon anatomy and structure

Composition:

The tendons of the body are an important part of a complex mechanic unit with the muscles. They consist of connective tissue which must have a certain density, as it connects the muscle and the bone to allow the muscles to transform contraction into locomotion. The majority of collagen in the tendons extracellular matrix is classified as collagen type I with a minority of types III, IV, V and IV. (44) In the extracellular matrix, the tendon cells, collagens and proteoglycans (mostly decorin but also hyaluronan, biglycan, fibromodulin and lumican) serve as organizers and lubricators to assemble the fibrils of the tendon. (45, 46) There is a hierarchical way in which tendons are organized (Figure 2). It starts with the orientation of the type I collagen, which is always parallel to the mechanical axis of the tendon and are organized as microfibrils in triple-helix polypeptide chains. Multidirectional stacking of these microfibrils forms the fibrils which are arranged to form the collagen fibers. (44, 46) Those fibers are loosely packed together with connective tissue called endotenon (see Figure 4). Fibers then combinate to form fascicles which are enclosed with a layer of epitenon to assemble the whole tendon. (46). The blood and lymphatic vessels, along with small nerves run in the loosely packed endotenon. (47)

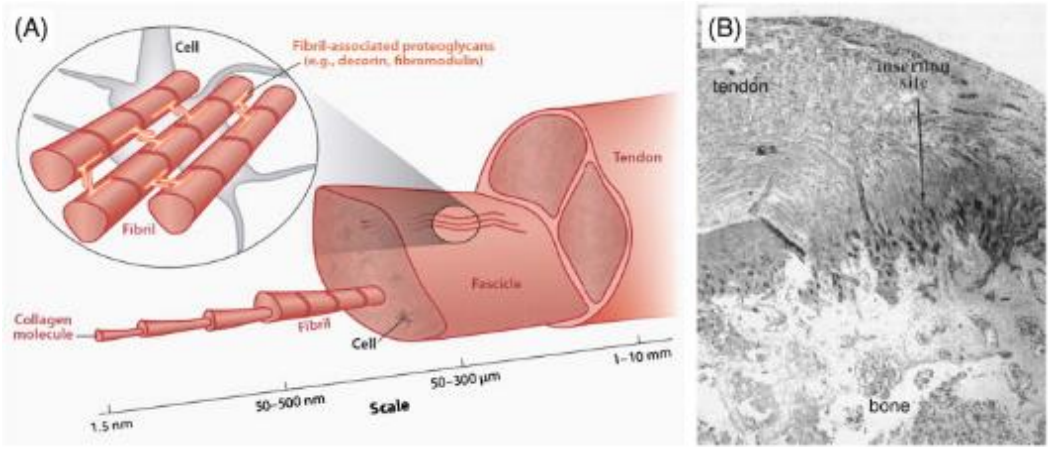

Figure 3: "Hierarchical structure of tendon spanning from the single collagen molecule up to fibrils, fascicles, and whole tendon. Inset image describes the structure of fibril-associated proteoglycans, the most abundant of which is decorin in tendon. (B) Histological section (4 ×) of the rat supraspinatus tendon-to-bone insertion site, highlighting the transition zone." Imaging of Connizzo et al. (46)

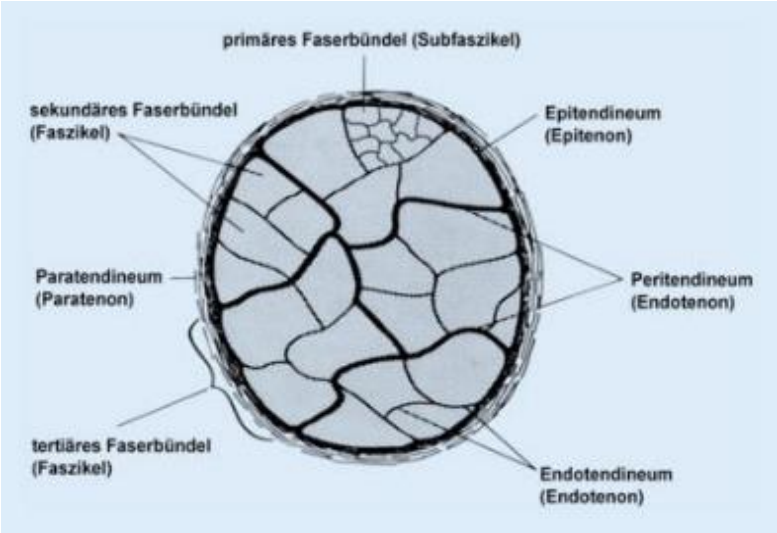

Figure 4: A schematic cross-section of a tendon. Picture taken from Zschäbitz, A: : Anatomie und Verhalten von Sehnen und Bändern. (47)

Entheses:

The part of the tendon where it inserts into the bone is called the enthesis and is of great clinical importance as it must withstand great forces to allow movement to the body. One can divide the type of entheses in two forms, fibrous and fibrocartilaginous. In fibrous entheses the tendon connects to the periosteum with insertion to meta- or diaphysis, also called indirect insertions. In contrast to that, the fibrocartilaginous entheses directly connect to the epiphysis or apophysis (see Figure 3). There exist four transitional zones which are labelled as: **1** dense fibrous connective tissue **2** uncalcified fibrocartilage **3** calcified fibrocartilage and **4** the bone (48).

Fibrous entheses are associated with e.g. the deltoid and some of the femoral muscles, which are accounted to the most powerful muscles in the human body. The entheses can be further divided into bony and periosteal, inserting either directly into the bone or taking an indirect course with primarily inserting into periosteum which then connects the tendon to the bone. This ensures a spreading of the force which is transmitted from the tendon to reduce stress but also limits the range of motion of the tendon, resulting in an inevitably short length of the tendon. (48)

Mechanosensitivity:

Because of the tendons distinctive hierarchical structure, their biomechanic function is highly potent. Tendons can be roughly divided into those who transmit loads (like the Achilles' tendon) and others who allow motion like flexor tendons of the hand. Elasticity and strength empower them to support the movement of muscle. Tendon anatomy and biomechanics vary vastly depending on the muscle and its function. Another characteristic of tendons is that they are mechanoresponsive, which means they can adapt their structure and function to the individual requirements for the tendon. (49)

Scleraxis, Mkx (Mohawk) and Egr1 (early growth response gene 1) are seen as the most important transcription factors of tendons respond to mechanical stimulation. Chen et al. showed in 2012, that the expression of Scleraxis and mechanical stress showed a synergistic effect on the induction of collagen fibril arrangement and an increased collagen fibril diameter ((25.04±1.76 nm *vs.* 21.2±1.7 nm, $p<0.05$)). (50)

3.6 Tenocytes

Tenocytes, which are fibroblast-like cells, are the main mature cell type which is found in ligaments and tendons. (51) They are linearly arranged between the collagen fibers (see figure 5) and are traversed by a network of stress fibers, composed of actin and myosin filaments, which extend through cell extensions to neighboring tenocytes. (47) Building the extracellular matrix, tenocytes play a fundamental role in the function of tendons as they adapt and react to given mechanical stimuli. Networking via tubular cell extensions with the help of gap-junctions allows them to communicate. As the tendon ages, the morphology of tenocytes changes as the cells are decrease in volume and number. Various markers and molecules expressed by tenocytes such as the transcription factor Scleraxis, which is essential in the process of adapting to mechanical stress were identified. Still, Scleraxis is expressed in the development of other mesenchymal tissue. (52) Tenomodulin, whose expression is induced by Scleraxis, regulates the proliferation and helps maturing the fibrils. (53, 54) Upon mechanical stimulus, Tenascin is expressed by tenocytes, but is also expressed by bones, smooth muscle cells and fibroblasts. (55)

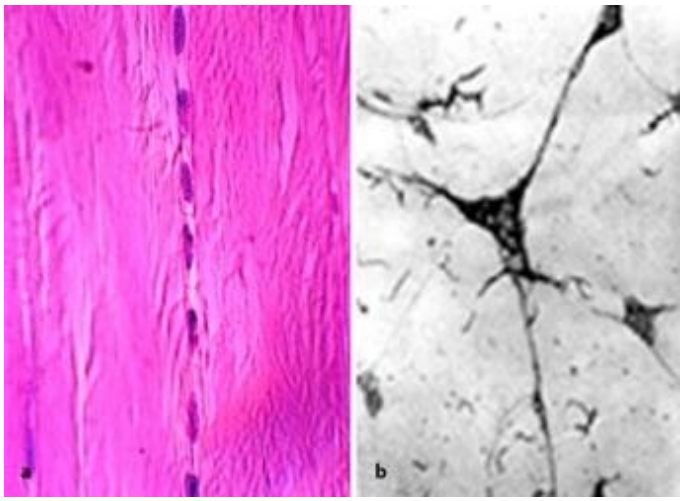

*Figure 5: **a** linearly arranged tenocytes **b** tenocytes and their cell extensions. Picture taken from Zschäbitz, A: Anatomie und Verhalten von Sehnen und Bändern. (47)*

3.7 Tendon regeneration

Tendons repair mechanisms and regeneration are special as the tendons tissue is mostly avascular. (51) Although tendons can withstand significant forces (tensile strength of tendons and ligaments range from 50 to 100 N/mm²), injury of the tendon, as it occurs in fractures, wounds or degeneration promotes scarring, limiting the tendons mobility and strength. (47) The excess of disorganized ECM disposition is called fibrosis. Fibrous scars lead to a decreased range of motion and cause pain to the patient. The most injured tendons are the flexor tendons of the hand, the tendons of the rotator cuff and the Achilles tendon. (56, 57) In severe cases, the fibrosis can lead to contractures of a joint if it results in a shortening of the muscle-tendon apparatus.(58)

Healing of tendons happens in three overlapping stages (see figure 6)

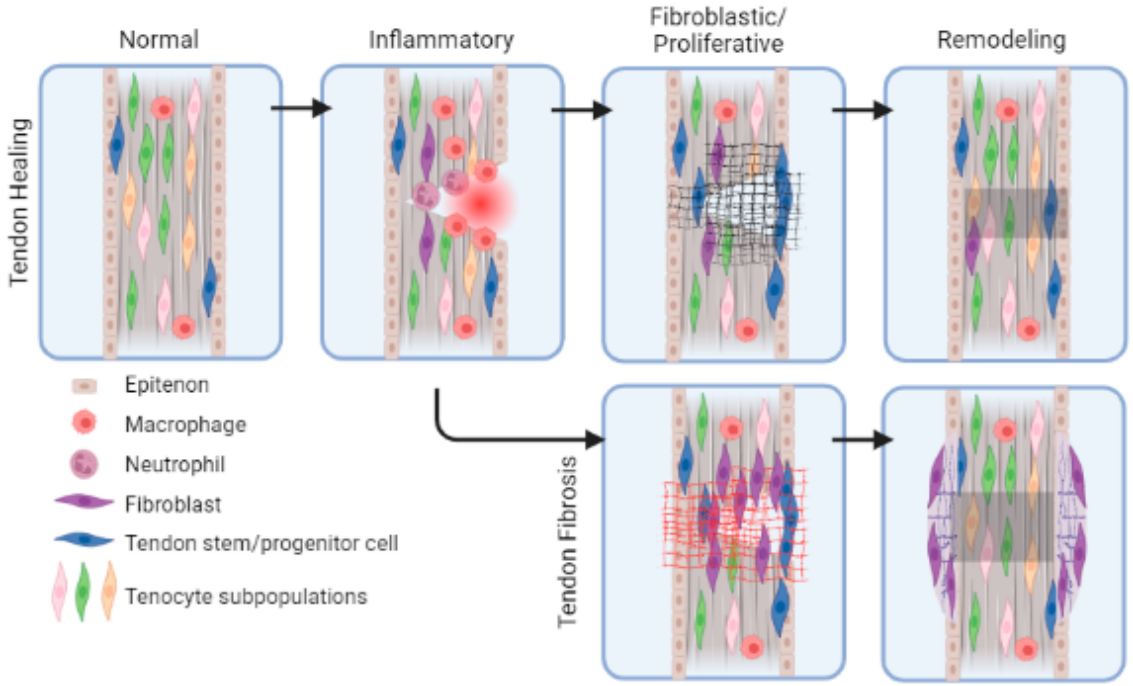

Figure 6: Different stages of healing and fibrosis of tendons and involved cells. Picture taken from Dilorio et. al : Understanding Tendon Fibroblast Biology and Heterogeneity (56)

The first stage of healing is the inflammatory stage. Lasting from approx. d1 to d7, it involves migration of thrombocytes, erythrocytes, fibroblasts and immune cells to the center of injury. As an immune reaction, phagocytosis of necrotic injured tissue is performed by neutrophilic granulocytes. This process takes place in the first 24h of injury. Afterwards, phagocytosis by macrophages occurs. Between d3 and d14, the fibroblastic/ proliferative phase starts by proliferation of fibroblastic cells. As seen in figure 6, a scaffold composed of collagen type III is formed for migrating cells and new tissue. The last stage is the remodeling phase. Starting approx. at d10, lasting up to several years, collagen type III is replaced by collagen type I. To increase the strength and elasticity of the ECM, fibers are crosslinked. (56)

Many growth factors are involved in the healing process of tendons. The chart below summarizes the involved cell types and growth factors and gives an overview of the processes of healing in the different phases.

Growth factor / Cell Type	Function	Phase of Healing
Tendon stem /progenitor	Differentiation to mature tendon cells (tenocytes)	All phases
Thrombocytes	Healing of blood vessels of the injured tendon, express PDGF	Inflammatory
Neutrophils	Phagocytosis of necrotic tissue	24h after injury
Erythrocytes	Injured blood vessels	Inflammatory
Macrophages	Phagocytosis, expressing growth factors stimulating fibroblasts, ↑ synthesis of ECM ↓ ECM degradation	Inflammatory
Fibroblasts	1. Migrating to injury 2. Depositing collagen type III 3. Depositing collagen type I	Inflammatory Proliferative Remodeling
Tenocytes	Collagen formation and intrinsic healing	All phases
PDGF (platelet derived growth factor)	Induction of synthesis of IGF-I and IGF receptors, stimulation of collagen, DNA and protein production + macrophage synthesis	Inflammatory and remodeling
IGF-I (insulin-like growth factor)	Stimulating formation of ECM, migration and proliferation of fibroblasts and tendon stem cells	Inflammatory and proliferative
VEGF (vascular endothelial growth factor)	Promotion of angiogenesis	Proliferative and remodeling
TGF β (transforming growth factor-beta)	Multiple functions, collagen production, promoting expression of Scleraxis, cell viability	All phases
bFGF (basic fibroblast growth factor)	Angiogenesis, proliferation and cellular migration, expression of other growth factors	All phases
MMP's (matric metalloproteinases)	Degrade and turn over collagen III to I, glycoproteins and proteoglycans	All phases

Chart 3: Key cells and growth factors, modified from Dilorio et. al: Understanding Tendon Fibroblast Biology and Heterogeneity. Biomedicines. (56)

3.8 Intrinsic vs. extrinsic fibroblasts

Healing of tendon tissue is achieved by extrinsic and intrinsic fibroblasts. The tenocytes account as intrinsic fibroblast and extrinsic fibroblasts are those who migrate to the site of injury. (59-61)

The extrinsic fibroblasts involved are located in the synovia and the tendon sheath and are one of the involved cell types of ECM production. (62) Multiple markers are associated with fibroblasts like vimentin, CD34 and PDGF receptor alpha. One can identify activated fibroblasts by the expression of aSMA (alpha smooth muscle actin). (63, 64)

The growth factors and specifics of tenocytes are described above in chart 3. In contrast to fibroblasts, tenocytes express tenomodulin (TNMD) and Scleraxis (Scx) which is used as a marker of tendon progenitor cell populations. (64, 65)

3.9 Fibroblast Heterogeneity

It was shown that there is a certain heterogeneity to fibroblasts as multiple subpopulations were identified. The number of these varies, depending on the origin and factors like injury status and data clustering methods. (56)

For example, Micheli et al. performed single-cell RNA sequencing (scRNA-seq) on intact Achilles Tendons of mice and identified three subpopulations of fibroblasts based on the expression of a component (Col1a1) of collagen type I. They also found that the typical tendon markers like TNMD, Scx and Mkx were not expressed across all the tendon fibroblast subpopulations, stating that there is no universal marker for tenocytes. (66)

On the other hand, Kendal et al. also used scRNA-seq and CITE-seq (cellular indexing of transcriptomes and epitopes sequencing) on human tendons (injured and non-injured) and identified five subpopulations of tenocytes. These subpopulations were defined by microfibril-associated proteins such as KRT7/SCX+, pro-inflammatory markers (PTX3+), pro- fibroadipogenic progenitors (APOD+), chondrogenic cells (TPPP3/PRG4+) and smooth muscle mesenchymal cells (ITGA7+).

Despite of the variety in the samples, all five of the above where present in injured and non-injured tendon tissue. The proportion of these subgroups remains unclear. (67)

Still et al. and Guo et al. also identified progenitor cell populations which were involved in tendon healing, including pro-inflammatory and mechanically responsive populations. (68, 69)

Tenocyte-related clusters, fibro-adipogenic progenitors and TPPP3+ tendon stem cells which are capable to differentiate into tenocytes were detected by Harvey et. al. in the sheath of the tendon. Identification of tenocytes was acquired on the expression of Fibromodulin, Tenomodulin and Thrombospondin 4. These cells were found to be able to renew themselves. (70)

Overall, this suggests that a standardized classification of tenocytes has not yet been established.

3.10 Tendon fibrosis

Like previously described, the healing process of tendons underlies three stages and is prone to difficulties due to its low vascularity as well as cellularity.

In the remodeling phase, a scar builds at the site of the injury. Intrinsic and extrinsic fibroblasts migrate to the injured part and fibrosis occurs due to an imbalance of these cell types. (60, 62) The healed part always has compromised mechanical as well as structural properties. (6, 57)

Fibrotic tissue between the surrounding tissue and the tendon itself is called an adhesion. It is estimated, that approx. 30% of tendon injuries heal with consecutive adhesion. (71) The adhesion limits the gliding motions of tendons, especially when it occurs in the flexor tendons of the hand presenting a huge impact on the range of motion of the underlying joint. Due to limited vascularity in the synovium, adhesions are more likely to form when intrasynovial tendons (e.g. hand flexors) are injured, in contrast to extrasynovial tendons (e.g. Achilles tendon). (57) Adhesion in the tendon can also cause pain to the patient in addition to impaired movement making it necessary to release adhesions surgically. (72) Figure 7 exemplarily shows the extensor tendons of the hand to highlight the anatomical proximity to osteosyntheses.

Figure 7: Extensor tendons on the back of the hand: 1 tendon of the M. extensor digitorum with intertendinous connection, 2 extensor retinaculum for the fixation of the 6 dorsal tendon compartiments. Picture taken from Zschäbitz, A: Anatomie und Verhalten von Sehnen und Bändern. (47)

There are different approaches to prevent adhesions forming in the healing process. Physical rehabilitation process was optimized by identifying that complete immobilization after tendon repairing leads to more adhesions. Passively moving the tendon as well as allowing partial motion reduces the formation of adhesions. (57, 73, 74)

Complete elimination of adhesion could yet not be achieved by optimizing physical therapy. Biomaterials, as well as biomedical engineering strategies are at the center of interest to prevent postoperative adhesion formation.

4 Materials and Methods

4.1 Materials

4.1.1 Chemicals

In the following chart, the chemicals used in this work are listed:

Chemicals	Manufactured by
Thiazolyl Blue Tetrazolium	Sigma Aldrich, St. Louis, US
Dimethylsulfoxid Hybrid-Max	Sigma Aldrich, St. Louis, US
Isopropanol	Carl-Roth GmbH, Karlsruhe, Germany
PBS (Dulbecco's Phosphate Buffered Saline)	Sigma Aldrich, St. Louis, US
Paraformaldehyde 4%	Gibco Invitrogen Life Technologies, Carlsbad, US
Triton X-100	Sigma Aldrich, St. Louis, US
Collagenase Type I 0.2 % and 0.5%	Worthington Biochemical Corporation, Lakewood, US
Hoechst Dye	Sigma Aldrich, St. Louis, US

Chart 4: Chemicals used and corresponding manufacturers

4.1.2 Devices

In the following chart, the devices used in this work are listed:

Devices	Manufactured by
Centrifuge Eppendorf 5804	(Eppendorf, Hamburg, Germany)
EVOS Digital Inverted Microscope	Life Technologies, Carlsbad, US
Incubator HERAcell 240 and B6 Function line	Heraeus Thermo Scientific, Waltham, US
Autoklav Systec DX-45	Systec GmbH, Wettenberg, Germany
Cell Counter, Luna automated cell counter, L1001	Nexcelom Bioscience LLC, Lawrence, US
FACSVia Flow cytometer	BD, Franklin Lakes, US

Chart 5: Devices used and corresponding manufacturers

Laminar Air Flow:

When working with cell culture, it is crucial to create as aseptic an environment as possible. The laminar air flow workstation ensures a low germ working atmosphere through its ventilation system. The utensils used in cell culture, such as culture flasks, cell culture plates, and pipettes, were all sterilized and packaged. Tweezers and other instruments used for the experiments were autoclaved in the laboratory.

4.1.3 Disposable materials

In the following chart, the disposable materials used in this work are listed:

Disposable materials	Manufactured by
Cell culture flasks sizes 25cm^2/75 cm^2/ 175 cm^2	Greiner Bio-one, Kremsmünster, Austria
Cell culture plates (24-Well Plates, 96-Well Plates)	Greiner Bio-one, Kremsmünster, Austria
Disposable pipettes 2ml/5ml/10ml/25ml	Corning Inc., Corning, US
Nalgene Cryotubes	Thermo Fischer Scientific Inc. Waltham, US
Luna Cell counting Slide	Nexcelom Biosciense LLC, Lawrence, US
Pipette Tips 10µl/200 µl/1000 µl	Starlab International GmbH, Hamburg, Germany
Sterile nylon filter, 70 µm	BD Biosciences, Franklin Lakes, US

Chart 6: Disposable materials used and corresponding manufacturers

4.1.4 Cells

In the following the cell lines used in this work are listed:

NHDF (NHDF, Promocell, Heidelberg, Germany):

This represents the primary cell type of connective tissue, which is involved in the maintenance of the extracellular matrix and plays a crucial role in the wound healing process.(75)

Tenocytes I and II (isolated from donor material):

The tenocytes utilized in this study were isolated from donor tissue. There was a consent form from the patients. Furthermore, there is an agreement between the Ethics Commission of the State Medical Association of Mainz and the University Medical Center regarding the use of donor material in research. Tenocytes are the defining cells of tendons and create a complex network by communicating cell extensions.(52)

L929 (ATCC, Manassas, US):

L929 are cell lines from fibroblasts of the connective tissue of mouses. Because of their ability to proliferate rapidly, they are often and regularly used in cell biology.

4.1.5 Cell medium

In the following the cell medium used in this work is listed:

NHDF/Tenocytes and L929: DMEM/ F-12 + GlutaMax (Gibco®, Life Technologies, Grand Island, NY, USA) + 10% FCS (Biochrom AG, Berlin, Germany) and 1% Penicillin/Streptomycin (Sigma-Aldrich, St. Louis, US)

4.1.6 Antiadhesive coatings – Polymers

In the following chart, the antiadhesive coatings are presented:

The polymers used for this work were created in the Department of Chemistry and Biology, Macromolecular Chemistry in Siegen, Germany

Polymer Coatings	Structure
A	Poly[$(HEAm)_{93}$-co-$(APAm)_5$-co-$(BPAm)_2$] side chain: amines
B	Poly[$(HEAm)_{93}$-co-$(AEAm)_5$-co-$(BPAm)_2$] side chain: amines
C	Poly[$(HPAm)_{93}$-co-$(APAm)_5$-co-$(BPAm)_2$] side chain: amines
D	Poly[$(HPAm)_{93}$-co-$(AEAm)_5$-co-$(BPAm)_2$] side chain: amines
E	Poly[$(HEAm)_{74}$-co-$(HPAm)_{24}$-co-$(BPAm)_2$] side chain: hydroxyl group
F	Poly[$(HEAm)_{49}$-co-$(HPAm)_{49}$-co-$(BPAm)_2$] side chain: hydroxyl group
G	Poly[$(HEAm)_{24}$-co-$(HPAm)_{74}$-co-$(BPAm)_2$] side chain: hydroxyl group
H	Poly[$(HEAm)_{93}$-co-$(AaAm)_5$-co-$(BPAm)_2$] side chain: carboxyl group
I	Poly[$(HEAm)_{93}$-co-$(AaAm)_5$-co-$(BPAm)_2$] side chain: carboxyl group
J	Poly ($HEAm_{98}$- co-$BPAm_2$) – free radical polymerization
K	Poly ($HPAm_{98}$- co-$BPAm_2$) – free radical polymerization
L	Poly ($HEAm_{74}$-co-$HPAm_{24}$-co-$BPAm_2$) – free radical polymerization
M	Poly ($HEAm_{24}$-co-$HPAm_{74}$-co-$BPAm_2$) – free radical polymerization

N	Poly ($HEAm_{98}$- co-$BPQAAm_2$) – free radical polymerization
O	Poly ($HPAM_{98}$-co-$BPQAAM_2$) – free radical polymerization
P	Poly ($HEAm_{74}$-co-$HPAm_{24}$-co-$BPQAAm_2$) – free radical polymerization
q	Poly ($HEAm_{49}$-co-$HPAm_{49}$-co-$BPQAAM_2$) - free radical polymerization

Chart 7: Polymer coatings

4.1.7 Antibodies used for immunofluorescence

In the following chart, the antibodies used in this work are listed:

Antibodies	Manufactured by
Scleraxis (A-7): sc-518082	Santa Cruz Biotechnology, Heidelberg, Germany
CNN1- Mouse Calponin-1 monoclonal antibody 0,1mg	Biozol Diagnostica Vertrieb GmbH, Eching, Germany
Anti- TNMD antibody Rabbit anti-human, Mouse TNMD Polyclonal Antibody	Biozol Diagnostica Vertrieb GmbH, Eching, Germany
Secondary Antibody goat-anti-mouse IgG Alexa 488	Invitrogen Life Technologies, Carlsbad, US
Secondary Antibody goat-anti-rabbit IgG H+L	Invitrogen Life Technologies, Carlsbad, US

Chart 8: Antibodies and corresponding manufacturers

4.1.8 Microbiology

In the following chart, the materials for microbiology are listed:

Materials	Manufactured by
BD BBL Prepared Plate Media: Trypticas Soy Agar	Thermo Fisher Scientific Inc., Waltham, US
Thermo Scientific Culti-Loops, Staphylococcus aureus subsp. Aureus ATCC 29213	Thermo Fisher Scientific Inc., Waltham, US
Müller Hinton Agar	Thermo Fisher Scientific Inc., Waltham, US
Mc Farland Standard 0,5	Carl-Roth GmbH, Karlsruhe, Germany

Chart 9: Materials used for microbiology and corresponding manufacturers

Methods

4.2 Methods

4.2.1 Isolation of tenocytes

Tenocytes used for this work were isolated from tendon donor material which would otherwise have been discarded. There was a consent form each patient. Furthermore, there is an agreement between the Ethics Commission of the State Medical Association of Mainz and the University Medical Center regarding the use of donor material in research.

Isolation procedure was done with modifications four times with successful isolation on the fourth try. In the first attempt, donor material was prepared on a sterile sheet, washed thoroughly with PBS and freed from access tissue like fat and muscle. The tendon was cut into pieces of approximately 3-4mm and placed in different wells of a 24-well plate. 2000 µL of Collagenase Type I with a concentration of 0.2% was added to the medium (DMEM/ F-12 + GlutaMax (Gibco®, Life Technologies, Grand Island, NY, USA) + 10% FCS (Biochrom AG, Berlin, Germany) and 1% Penicillin/Streptomycin (Sigma-Aldrich, St. Louis, US)). Collagenase digestion lasted for 16h until the next morning at 37°C with 5% CO_2. Medium was filtered with a 70µm sterile filter and centrifuged for 5 minutes with 1400rpm. Cell pellet was resuspended and seeded into wells on a 24-well plate and covered with medium. No cells were adherent to the cell culture plates with this method.

In a second attempt, concentration of Collagenase Type I was increased to 0.5% and the culture plate was incubated on a rotating plate. Again, no cells were adherent to the culture plate. Third attempt was identical, except for incubating in a 6-well plate instead of a 24-well plate.

For a successful isolation of tenocytes, the tendons were prepared as described above. Tendon fragments were incubated with medium, containing 10% FCS and 25µ/ml ascorbic acid for several days. Tenocytes started to migrate from the tendon fragments and started to adhere to the wells of a 6-well plate. By the time a confluence was reached, cells were transferred to a cell culture flask. Two cell lines, referred to as Teno 1 and Teno 2, were isolated.

4.2.2 Cell preservation (Freezing)

To preserve the cells, they are stored in nitrogen. The cells need to be prepared as follows for freezing. First, the cells are centrifuged at 1400 rpm for 5 minutes. The resulting pellet is resuspended in FCS and 10% DMSO (Sigma-Aldrich, St. Louis, US). Special cryogenic tubes (Nalgene Cryotubes, Thermo Fischer Scientific Inc. Waltham, US) are filled with the cells and placed in a box, as they can withstand the extreme cold temperatures which are needed to reach cryopreservation. These are cooled at -80°C for 24 hours and then transferred to a nitrogen tank (Argpeg 110, Air Liquide S.A, Paris, France) at -196°C the following day.

4.2.3 Cell passaging

Cell cultures must be regularly split to prevent excessive growth in the culture flasks. Once a certain level of growth is reached, subculturing must take place. The cells are washed with PBS, and then Accutase (Sigma-Aldrich, St. Louis, US) (76) is applied to detach the cells; this process occurs at 37°C. After inspection under a light microscope, medium containing FCS is added to deactivate the Accutase. Centrifugation at 1400 rpm for 5 minutes forms a cell pellet, which is then resuspended and diluted in medium. This subculture is subsequently transferred to a new culture flask.

4.2.4 Immunofluorescence

To safely identify the isolated cells as tenozytes, they were examined immunohistochemically. Approximately 30.000 cells were seeded per well in a 24-well plate and incubated overnight. After securing a sufficient cell confluence under the light microscope, the cells were fixated with 500 µl of phosphate buffered saline with 4% of paraformaldehyde (PBS-PFA) and incubated at room temperature für 15 minutes. After washing with PBS with 0.5% of bovine serum albumin (BSA) two times, they were washed with 1% Triton-X100 buffer solution to permeabilize the cell membranes. Then, 250 µl of the primary antibodies in different concentrations (chart 7) were added to the wells and incubated at room temperature for two hours. After that, the cells were washed again with PBS-BSA and 250 µl of the secondary antibodies was added, which was then incubated at room temperate for one hour in a dark place. The next step was washing with PBS-BSA, then adding 250 µl of Hoechst dye with a concentration of

1:250 and incubating for another ten minutes. The cells were then regarded and photographed with EVOS digital inverted microscope and compared to a negative control. This experiment was done three times using different antibodies.

Antibodies	Concentration
Scleraxis	1:500 / 1: 50
CNN1	1:250
TNDM	1:100
goat-anti-mouse IgG AL488 for CNN1	1:100
goat-anti-rabbit IgG AL488 H+L for TNMD	1:500
goat-anti-mouse IgG H+L AL546	1:500

Chart 10: Concentration of antibodies

For the third experiment, Tenomodulin and CNN1 were combined and 125 µl each was added to avoid dilution. Secondary antibodies were also reduced to 125 µl each. Concentration remained constant.

4.2.5 Lentiviral transduction with eGFP

For better visibility of the cells, they are transduced with a viral vector containing eGFP (Georg Speyer House, Frankfurt, Germany). The enhanced green fluorescent protein is extracted from the Aequorea Victoria jellyfish and can generate an internal fluorophore which results in great visibility. Therefore its use in cell culture is long established. (77) The day before the transduction,10 x 25.000 cells are seeded in a 24-well plate. The medium is aspirated, and 500 µl of standard medium with a concentration of 5 µg per ml of protamine sulfate is added. The viral supernatant is diluted to a concentration of 1:10 (900 µl of medium and 100 µl of viral supernatant). Then, 100 µl of this solution are added to five wells, and 50 µl are added to the other five wells. After 6 hours, the solution is aspirated, and the cells are cultured overnight in medium with 20% FCS. The next day, the procedure is repeated, this time adding 100 µl to the other wells and vice versa.

4.2.6 FACS-Assay (Fluorescence Activated Cell Sorting)

To measure the efficacy and intensity of the transduction with eGFP, a FACS Assay was performed. Flow cytometer FACSVia (BD, Franklin Lakes, US) was used for measurements. FACS assay was done for both NHDF and tenocytes after transduction with eGFP.

To prepare the cells for FACS, they were detached from the cell culture flasks using Accutase which was then inactivated with medium + FCS. After that, the suspension was centrifugated at 1400rpm for 5 minutes. The supertenant was then removed and the cell pellet was resuspended with 6ml of medium. Cell counting with Luna automated cell counter. Per measurement tube, approximately 200.000 cells of NHDF/tenocytes were prepared. Afterwards, cell pellets were washed and resuspended using PBS-FCS two times in a row. The counted number of cells was then resuspended in 400 µl PBS each and then transferred to the FACS measurement tubes. Until the measurement took place, the tubes were packed in aluminum foil and transported on ice.

4.2.7 Cell viability (MTT Assay)

To examine the cytotoxicity of the different polymers, the MTT (3-(4,5-dimethylthiazol-2-yl)-2,5-diphenyltetrazolium bromide) assay was performed with L929 cells. Figure 8 shows a schematic overview of the MTT-Assay.

Day 1:

After counting the cells, approximately 10.000 cells per well were seeded in a 96 well plate and covered with standard medium and incubated overnight at 37 ° Celsius. In addition, medium was added to polymers which also incubated overnight. A row of medium without cells was set up for blank measurement.

Day 2:

The standard medium on the L929 cells was removed and medium with contact to polymers was added to each row. Standard medium was changed in the row for blank measurement, one row of L929 cells received standard medium as a reference.

Day 3:

The day of measurement, the Thiazolyl Blue Tetrazolium salt was diluted in medium without FCS to create solution with a concentration of 1%. 20 µl were added to each well and were then incubated at 37°, 5% CO_2 for 3h. Then, after removing the MTT, 100µl of Isopropanol is added to extract the MTT from the cells. The absorption was measured at 570 nm (reference 650 nm) using a spectrophotometer (Tekan, Sunrise, Maennedorf, Switzerland). The experiment was repeated three times for each polymer.

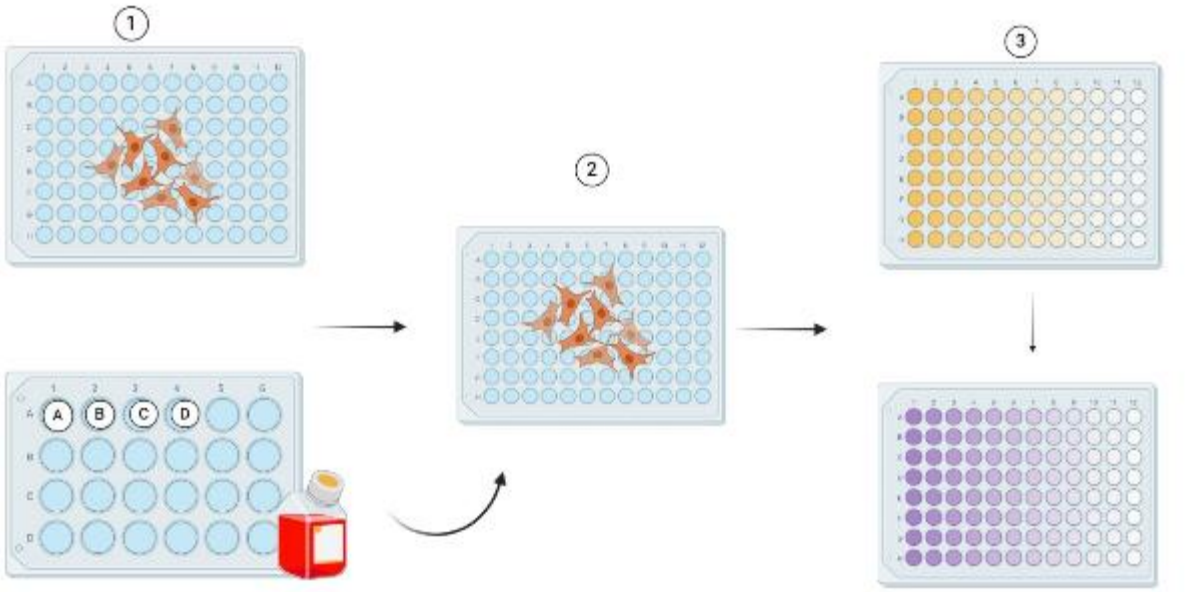

Figure 8: A schematic overview of the MTT-Assay (the figure was created using Biorender.com).

4.2.8 Cell seeding on coated plates

To examine the quality of antiadhesive characteristics of the different polymer coatings, the NHDF+ eGFP and tenocytes + eGFP were seeded on the coatings in 24-well plates. The plates were either fully coated (FC) or partially coated (PC) with the polymer to be tested. The FC wells contained 4mg/5mg of polymer per well whereas the PC contained 0.2mg/0.25mg droplets of polymer. The polymers were linked at a wavelength of λ= 365nm. In addition, every well-plate with coatings also had a row with the adhesion polymer (AP) which was also examined with both cell lines.

The well-plates were delivered from Siegen and stored frozen at approximately -18 °C. Preparing the plates for seeding, they were thawed at room temperature for 2h. The wells were washed twice with PBS before about 25.000 cells were seeded per well. 1000 µl of DMEM/ F-12 + GlutaMax (Gibco®, Life Technologies, Grand Island, NY, USA) + 10% FCS (Biochrom AG, Berlin, Germany) and 1% Penicillin/Streptomycin (Sigma-Aldrich, St. Louis, US) was added to each well.

Images of cell growth were taken with EVOS Inverted digital microscope at Day 1 (D1), Day 3 (D3) and Day 7 (D7). After one day, a secondary cell culture was segregated (see chapter 4.2.9) by taking 500 µl of medium, which was then refilled up to a total of 1000 µl. These experiments were repeated three times for each cell line (NHDF / tenocytes).

4.2.9 Cell culture from seeded cells

The aim of the secondary cell culture was to visualize the growth of cells which have been in contact with the polymer coatings for 24h. For this purpose, the medium was mixed thoroughly using a 500 µl pipette. After this step, 500 µl of medium (half of the medium) was taken and added to a new 24-well plate to examine whether the cells were still able to replicate.

Images of cell growth were taken with EVOS Inverted digital microscope at Day 1 (D1), Day 3 (D3) and Day 7 (D7). These experiments were repeated three times for each cell line (NHDF / tenocytes).

4.2.10 RNA Isolation and RT-PCR

RNA isolation:

To further characterize the tenocytes, RNA isolation was performed using peqGOLD Total RNA Kit. For this, Teno 1 and Teno 2 cells were detached from cell culture flasks and centrifuged to form a cell pellet. The cell pellet was frozen and stored at -80°C.

Lysis:

300µL of RNA lysis buffer was added to the cell pellet and was resuspended thoroughly and afterwards centrifuged at 10.000xg* for 1 minute.

Loading and binding:

Subsequently, 200 µL of 70% Ethanol was added and mixed, then pipetted on the PerfectBind RNA Column and centrifuged again for 1min at 10.000xg*. DNA Removing Column was discarded, and a new collection tube was taken.

Washing I:

Then, 500µL of RNA Wash Buffer I was added to the PerfectBind RNA Column and centrifuged again for 1 minute at 10.000xg*. Excess was discarded, collection tube was used for the following steps.

Removal of DNA with DNase:

Following mix was prepared and pipetted onto every PerfectBind RNA Column membrane:

70 µL of RNase-free Buffer RDD DNA Digest Buffer + 10 µL RNAse -free DNase I (Qiagen)

The mix incubated at room temperature for 15 minutes. The column was placed on a new collection tube and 400 µL of RNA Wash Buffer I was added. Another five minutes of incubation at room temperature following centrifugation for 5min at 10.000xg*. Exchange of the collection tube.

Washing II:

500µL of RNA Wash Buffer II were added onto the PerfectBind Column and centrifuged for 1min at 10.000xg*. This step was performed twice; collection tube was renewed.

Drying: PerfectBind Column was put into the empty collection tube. For drying, the tube was centrifuged for 2min at 10.000xg*.

Elution:

For elution, PerfectBind RNA Column was placed on a new collection tube. After that, 15 µL of RNase free dH_2O was pipetted onto the membrane. Centrifugation for 1 min at 6000g.

Quantifying the RNA:

To quantify the concentration and the purity of the extracted RNA, the absorption was measured at 260 and 280nm.

Measurements for tenocytes showed a ratio between 1.83 and 2.10 for Teno 1 and 1.05 and 2.07 for Teno 2.

Synthesis of cDNA:

The synthesis of cDNA or reverse transcription as achieved using the Thermocycler Peqstar 2X. Program M-MuLV-Rev. Tra.

Programs of the Thermocycler:

Heat Lid to 110°

5 min at 65 °

6 min at 25°

1h at 42° (replication)

20 min at 65° (inactivation of rev. transcriptase)

store at 4°

The first two steps of the program were performed using the following preparation:

2 µL of random primers (hexamers)

2 µL of dNTP (deoxynucleotide triphosphate)

y µL of RNA free water (volume depends on concentration of RNA. For each sample 1 µg of RNA was calculated). Water is added to create a total volume of 15 µL including the random primers and the dNTP.

X µL of RNA

After 5 minutes, following mix was added to each RNA sample:

2 µL 10x MuLV RevTra-Buffer

2 µL RNase free water

1 µL M-MuLV Reverse Transcriptase (BioLabs. M0235S, 10.000U= 200,000U/ml)

Mix was put back into the Thermocycler for Steps 3-5. The resulting cDNA was used for qPCR and stored at 4°C.

qPCR:

For teno1 and 2, the expression of the following genes was tested. GAPDH as housekeeping gene, Scleraxis, Tenascin, Tenomodulin and vWF (van Willebrand factor).

Primer	Sequence (5'->3')
hsScleraxis_for	CTCCAGCTACATCTCGCACC
hsScleraxis_rev	CGCGGTCCTTGCTCAACTTT
hsTenascin_for	TGGCATCGGAGAATGCCTTT
hsTenascin_rev	TCCGGTTCGGCTTCTGTAAC
hsTenomodulin_for	AATGAACAGTGGGTGGTCCC
hsTenomodulin_rev	TTGCCTCGACGGCAGTAAAT
GAPDH_for	CGA CCA CTT TGT CAA GCT CA
GAPDH_rev	AGG GGA GAT TCA TGT TGG TG
vWF_for	GGA TTC AGT GGA TGC AGC AG
vWF_rev	TAG GGA GGT CTT CGA TTC GC

Chart 11: Primers used and their sequences from 5'->3'

Following mix was pipetted for each gene:

4,8 µL of RNase free water

0,1 µL of forward primer

0,1 µL of reverse primer

10 µL SyBr. Mix (Biozym, Hamburg, Germany)

PCR mix was pipetted in each well and 5 µL of cDNA was added. RNase free water served as control. PCR was started with following program:

Repetition	°C	m:s
40x	95	02:00
	95	00:05
	60	00:25

Chart 12: program for qPCR

4.2.11 EVOS-Microscopy and Photography

EVOS (Electronic Vision Optical System) microscopy was used to visualize and photograph the NHDF and tenocytes which were transduced with eGFP. The EVOS microscope is equipped with the ability to depict multiple wavelengths, making it a useful tool also in microscopy of immunofluorescent cells.

<u>The wavelengths used for this work were:</u>
GFP: 470nm excitation and 525nm emission wavelength
DAPI mode: 357nm excitation and 447nm emission wavelength
RFP: 531nm excitation and 593nm emission wavelength

Pictures were taken at different magnifications, marked in the lower right of every picture.

4.2.12 Microbiology

Day 1:

Culti-Loops with Staphylococcus aureus subsp. Aureus ATCC 29213 (Thermo Fisher Scientific Inc., Waltham, US) were diluted with 1000 µl of NaCl and then spread on Tryptic Soy Agar. Incubation at 37° C for 24h.

Day 2:

On the second day, two colonies of Staph. aureus were harvested and dissolved in 1000 µl of NaCl. An adjustment to the McFarland standard (Carl- Roth GmbH, Karlsruhe, Germany) was not necessary.
Two petri dishes with a diameter of 35mm coated with each 37.5mg of **J** (Poly ($HEAm_{98}$- co-$BPAm_2$)) and **N** (Poly ($HEAm_{98}$- co-$BPQAAm_2$)) were washed with PBS and then covered with 2000 µl of DMEM/ F-12 + GlutaMax (Gibco®, Life Technologies, Grand Island, NY, USA). A positive and a negative control was set up in a 6-well plate. Incubation at 37° C for 24h.

Day 3:

On the third day, a dilution series was set up. The medium was diluted to concentrations of:

1:1000

1:10.000

1:100.000

1:500.000

This experiment was conducted as a duplicate setup for each **J** and **N** with a positive control (dilution series as described above) and a negative control without bacteria.

100 µl of the diluted suspension was applied with a Drigalski-spatula on a petri dish containing Müller-Hinton agar (Thermo Fisher Scientific Inc., Waltham, US) according to the above-described scheme. Incubation for 24 hours, with photography taken on Day 4.

5 Results

5.1 Lentiviral transduction of tenocytes and fibroblasts

Figure 9 shows a photography of Tenocytes 1 and 2 before and after lentiviral transduction with eGFP. Before, the cells show good confluence and vitality. Five days after transduction, tenocytes are building confluence and a bright expression of the green fluorescent protein which was needed for following experiments.

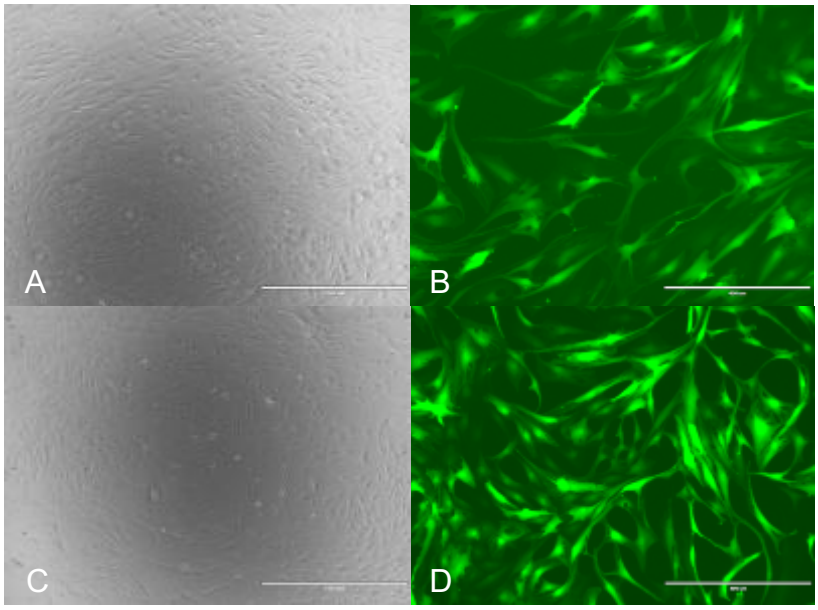

Figure 9: Tenocytes 1(A) and 2 (C)before and after lentiviral transduction with eGFP (B+D), Photography taken with EVOS

Below, one can see the transduction process of NHDF. After transduction the cells show strong expression of eGFP and viable cells with good confluence.

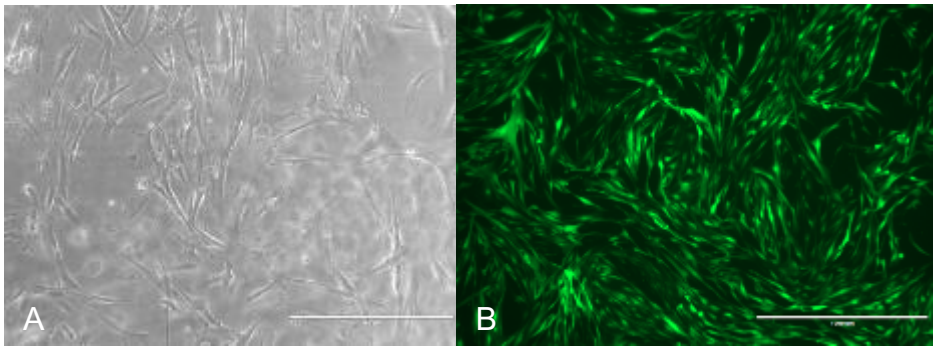

Figure 10: Fibroblasts before (A) and after transduction (B), Photography taken with EVOS, Scale 400µm and 1000µm

5.2 Immunofluorescence for characterization

5.2.1 CNN1 + Anti- TNMD

Calponin 1 acts as a marker of smooth muscle cells as it interacts with α-Actinin-Actin. It does not serve as a marker for tendon cells in general but is limited to the detection of vascular structures in tendons. Therefore it is of great use in immunohistochemistry. (78) Figure 11 shows the staining of Teno 1 with an overlay of Hoechst Dye indicating the expression of calponin 1 in these cells as well as in the Teno 2 cells.

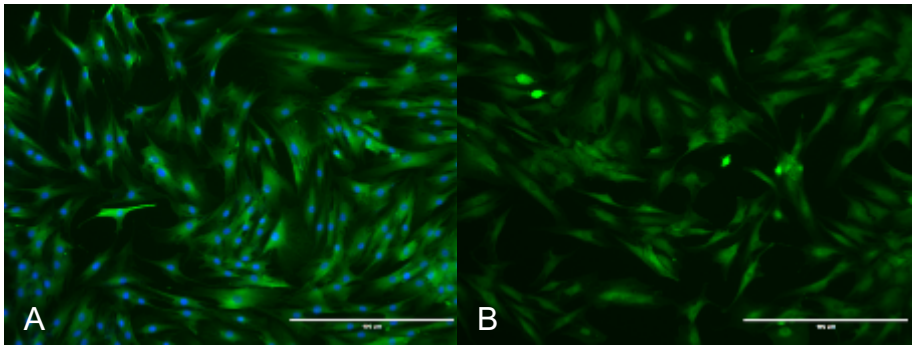

Figure 11: A: Immunofluorescence of Teno 1 with CNN1 and DAPI, Photography taken with EVOS, Scale 400µm, B: Immunofluorescence of Teno 2 with CNN1, Photography taken with EVOS, Scale 400µm

Another marker for characterizing tenocytes is Tenomodulin (TNMD), a transmembrane glycoprotein which is mostly expressed in dense connective tissue such as tendons and ligaments. (53) Figure 12 shows both Tenocytes 1 and 2 with expression of Tenomodulin, indicating its origin from tendon material. Nuclei were stained with Hoechst dye.

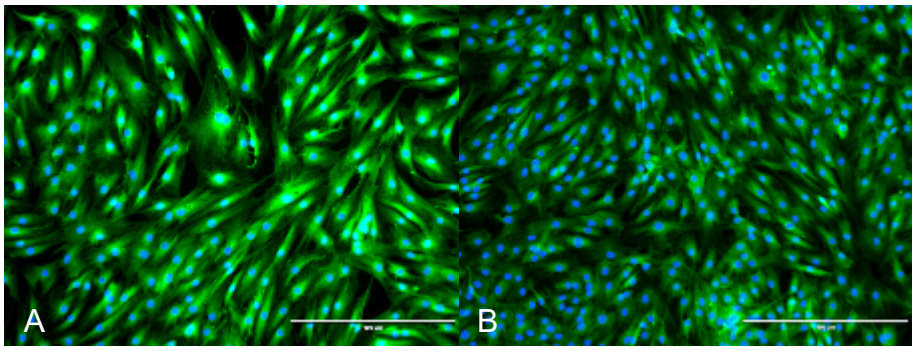

Figure 12: A: Immunofluorescence of Teno 1 with Anti-TNMD and DAPI, Photography taken with EVOS, Scale 400µm. B: Immunofluorescence of Teno 2 with Anti-TNMD and DAPI, Photography taken with EVOS, Scale 400µm

5.2.3 CNN1, Anti- TNMD and DAPI

Tenocytes 1 and 2 were also stained with both Calponin 1 and Anti-TNMD. Different secondary antibodies were used (red staining for CNN1 and green staining for Anti-TNMD) to highlight the different targets of immunohistochemistry. Figure 13 shows Tenocytes 1 and Tenocytes 2 with CNN1(+Hoechst) and Anti-TNMD (+ Hoechst).

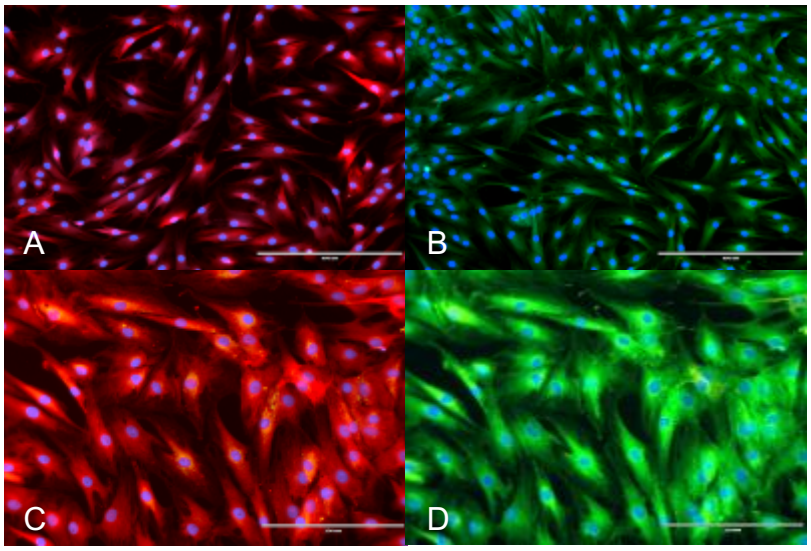

Figure 13: Immunofluorescence of Teno 1 with A: CNN1 and DAPI and B: Anti-TNMD and DAPI, Photography taken with EVOS, Scale 400µm, C: Teno 2 and CNN1and DAPI D: Teno 2, Anti-TNMD and DAPI

Figure 14 shows an overlay of CNN1, Hoechst nucleus dye and Anti-TNDM in Tenocytes 1 and Tenocytes 2, the combination of both markers and its presence in both Tenocytes 1 and 2 is highlighting their origin of mature human tendon material.

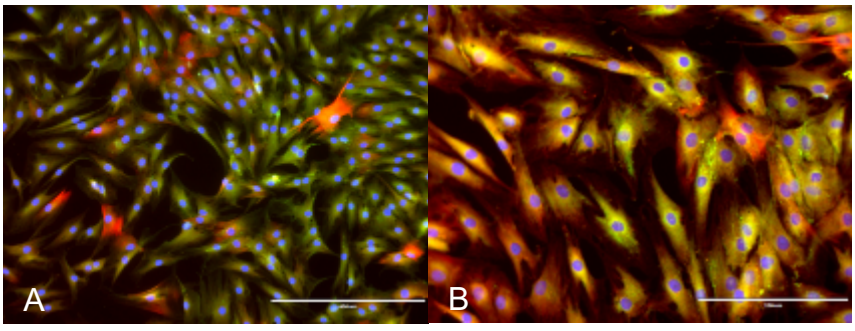

Figure 14: Immunofluorescence with CNN1, DAPI and Anti-TNMD A: Teno 1 and B: Teno 2, Photography taken with EVOS, Scale 400µm for A and 200µm for B

5.3 Transduction efficiency with FACS

To verify transduction efficiency, flow cytometry was performed. Tenocytes 1 and 2 as well as NHDF were analyzed in comparison to a non-transduced control of each cell line. The mean transduction efficiency of is shown in chart 13 below.

Cell Type	Efficiency
Teno 1	93.7%
Teno 2	95.1%
NHDF	70.5%

Chart 13: Transduction efficiency of the cell lines

For NHDF, a sufficient level of transduction was reached with >70% whereas a high transduction efficiency was reached for both tenocyte cell lines with > 93%.

Figure 15 illustrates the distribution of transduction efficiency. The x-axis represents FITC-A reflecting the intensity of fluorescence while the y-axis depicts the cell count.

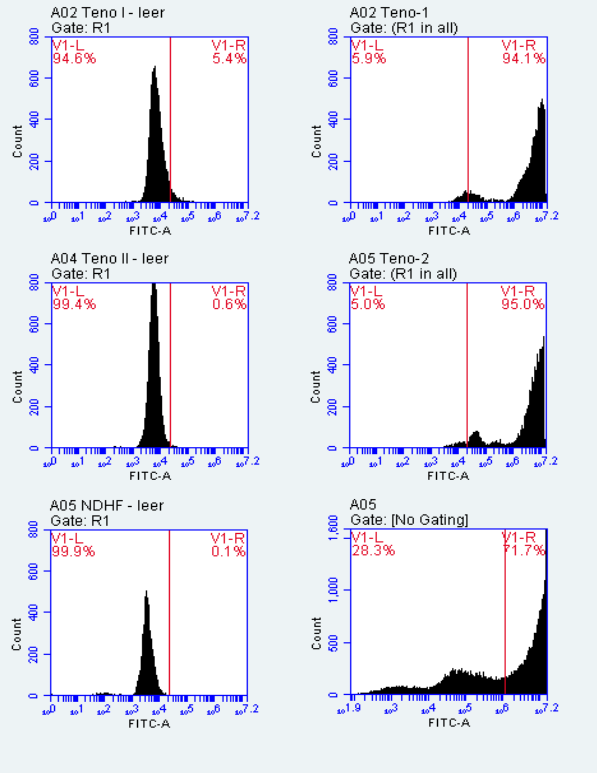

Figure 15 : FACS assay showing the transduction efficacy of Tenocytes and Fibroblasts

5.4 Cytotoxicity

Biocompatibility of the polymers is a very important aspect. Given that, the polymers were all tested in a MTT viability assay as they should prevent adhesion to the surrounding tissue without being cytotoxic. Chart 14 represents the results of the assays compared to a control which was set as 100%.

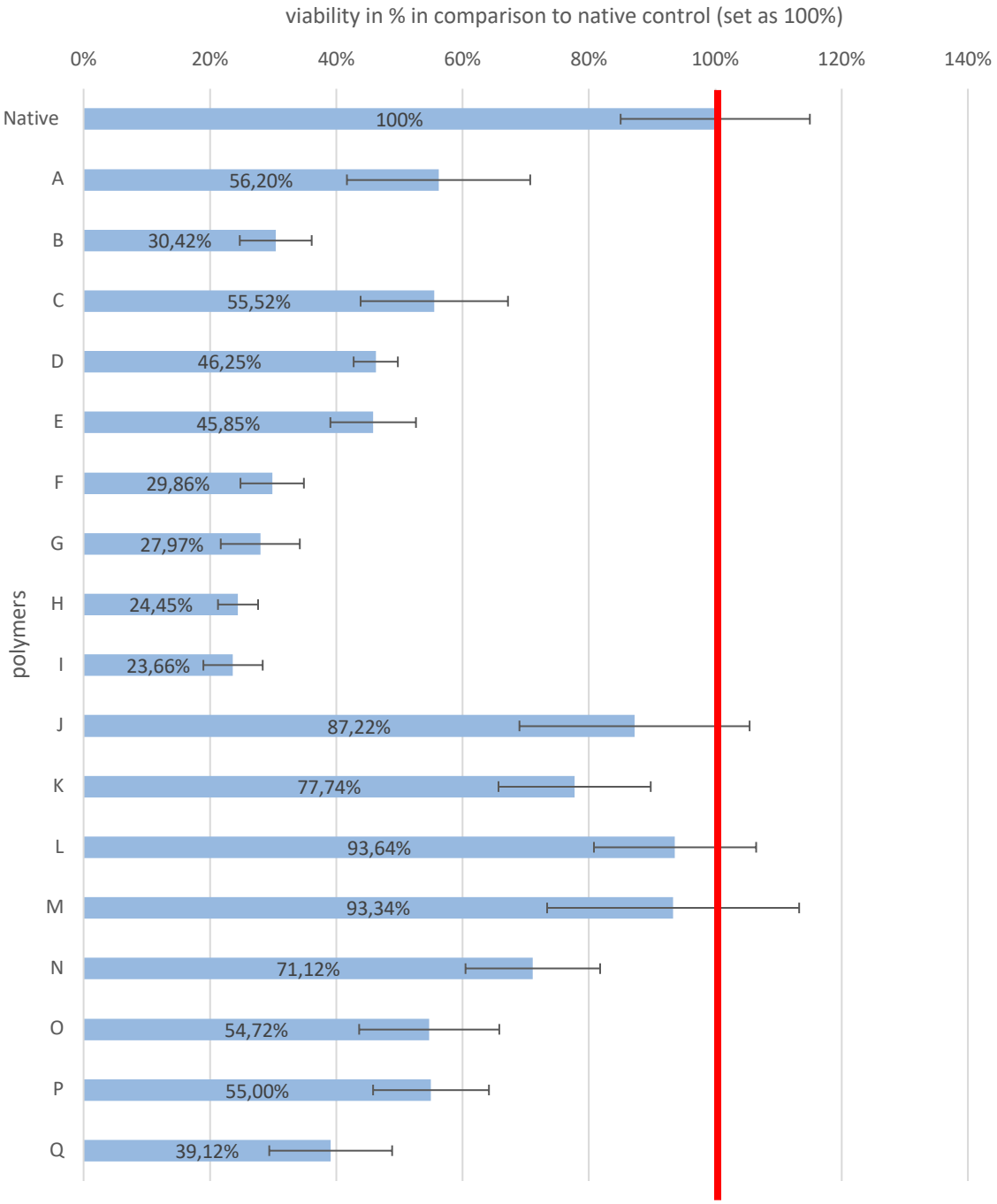

Chart 14: MTT Assay of all tested polymers with standard deviation. The red line marks the control which was set as 100%.

The results showed variable effects of the polymers on the cells as there is a range from 23.66% to 93.64% in cell viability.

The polymers can be roughly divided by their method of polymerization. As polymers A-I behold the end group from the RAFT polymerization, J-Q are prepared by free radical polymerization (FR).

Our results indicated that the polymers A-I created an overall more cytotoxic environment to the L929 murine cells than the polymers J-Q. Especially polymers B and E-I showed cell viability under 40% and were therefore rated not suitable for an in vivo use (RAFT group). Polymers J-Q of the FR group showed better results for cell viability; however, polymer Q also showed a percentage of under 40% and was therefore not suitable.

Polymer A seemed to show the least cytotoxicity of the RAFT polymers. Polymers L and M showed great viability of ~ 93% in the FR group, the others (J, K, N, O, P) all showed viability of >54 %.

Cytotoxicity was classified with its percentage compared to the positive control as following:

+++ -> 90-100 %

++ -> 80-90 %

+ -> 70-80%

- -> 60% - 70%

-- -> 50% - 60%

--- -> 40% - 50%

Chart 14 gives an overview of all tested polymers, the cytotoxicity and the in vitro testing with fibroblasts and tenocytes.

5.5 Cell growth on hydrogel coated plates:

5.5.1 Fibroblasts:

In the following figures, the **fibroblast** cell growth on polymer-coated plates is shown. All Figures show day 6/7 of growth on partially coated (PC) plates and fully coated (FC) plates. Images were taken on day 1, day 3 and day 6 /7, however the main interest is to ensure that there are no long-term adhesions forming which is the reason we chose day 7 to show the results. Growth was visualized in different magnifications with EVOS.

Figure 16 exemplarily shows an example of the course of all taken images and the growth on a PC plate.

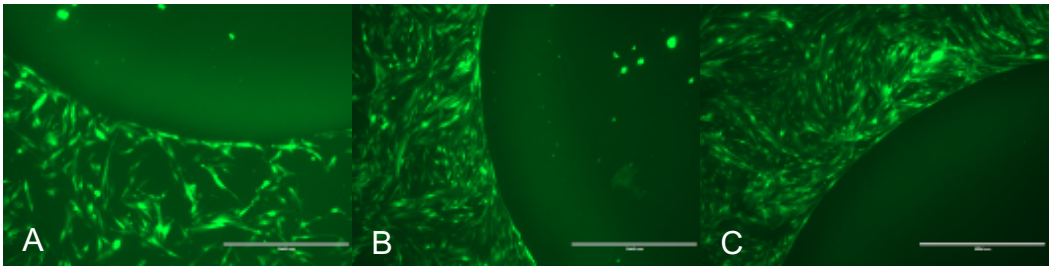

Figure 16: Example of imaging on d1 (A), d3 (B) and d7 (C) with polymer A

Furthermore, we had to classify the cell growth, so different categories were established. In some images one can clearly see differentiated cells, especially on the outer (non-coated) edges of the PC wells. On other images one can identify different stages of cell growth. Some cells are clearly differentiated with cell extensions; others were round and showed no signs of differentiation. With the following system, we tried to consider the different stages of cell differentiation and the number of remaining cells on the coatings.

+++ -> no adherent cells, only on the edges

++ -> cell debris, little

+ -> cell debris, much

- -> few cells but showing initial differentiation

-- -> many cells with initial differentiation

--- -> a lot of differentiated cells

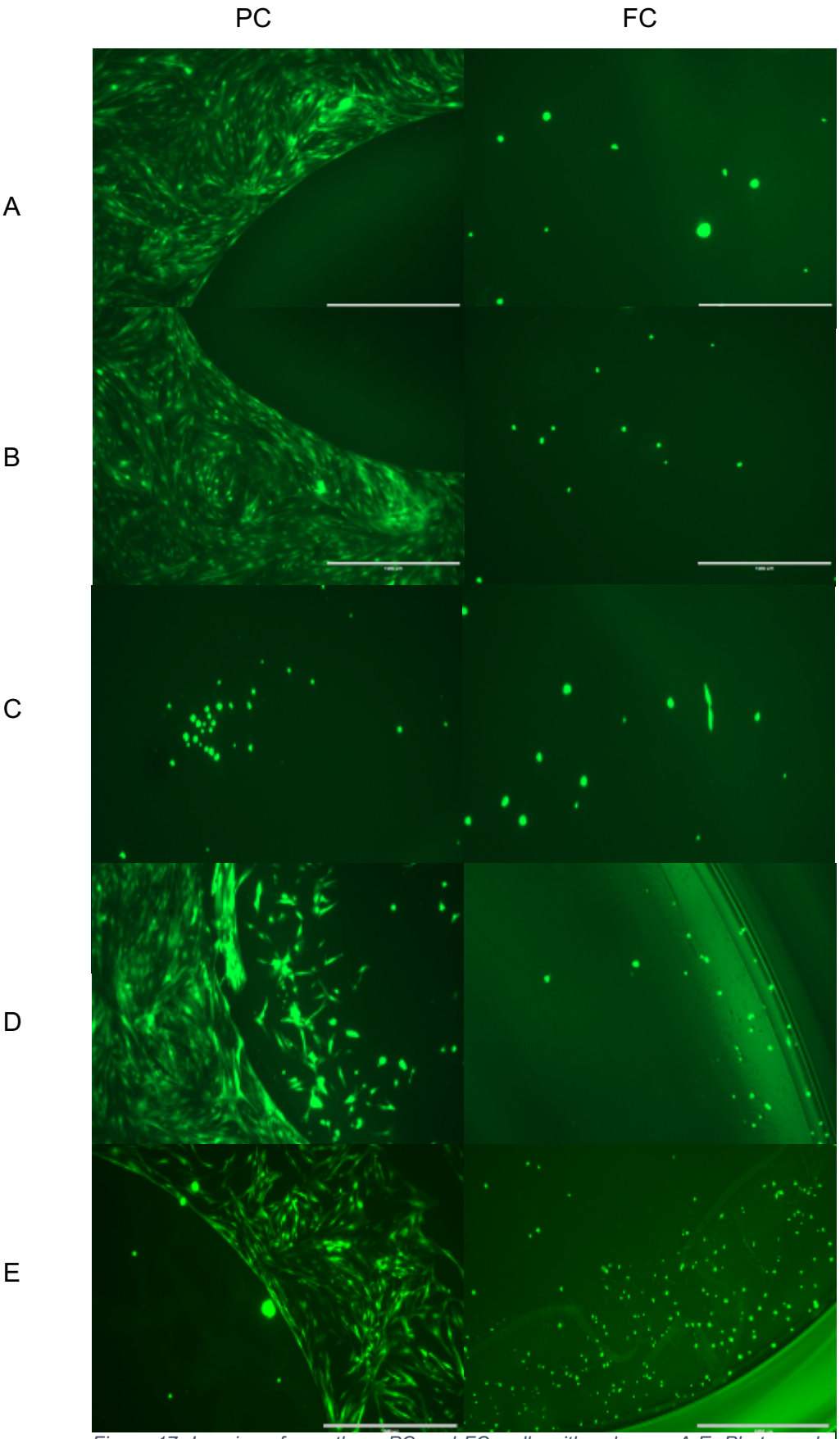

Figure 17: Imaging of growth on PC and FC wells with polymers A-E, Photography taken with EVOS in differing magnifications showing different amounts of cell growth

Polymer A: Poly[$(HEAm)_{93}$-co-$(APAm)_5$-co-$(BPAm)_2$], Side chain: Amine group

Polymer A was classified with +++ as there were a lot of viable cells on the edges of the PC wells but none / only very little cell debris on the coating of the FC well.

Polymer B: Poly[$(HEAm)_{93}$-co-$(AEAm)_5$-co-$(BPAm)_2$], Sidechain: Amine group

Polymer B was also classified with +++ as there was little to few cell debris whereas you can see the sharp edge of the coating on the PC well.

Polymer C: Poly[$(HPAm)_{93}$-co-$(APAm)_5$-co-$(BPAm)_2$], Side chain: Amine group

Polymer C was classified as ++ coating. One could see a sharp edge with few cell debris on the coating itself.

Polymer D: Poly[$(HPAm)_{93}$-co-$(AEAm)_5$-co-$(BPAm)_2$] , Side chain: Amine group

Polymer D was classified as a - - coating. One can see a sharp edge of the coating but on the coating itself there were many cells with differentiation which started to form a cell network.

Polymer E: Poly[$(HEAm)_{74}$-co-$(HPAm)_{24}$-co-$(BPAm)_2$] , Side chain: hydroxyl group

Polymer E was classified as ++/+++. There was a good cell network forming on the edge of the PC well but also few cell debris in the PC. The FC wells showed no differentiated cells and no network but there was cell debris on the edges of the coatings.

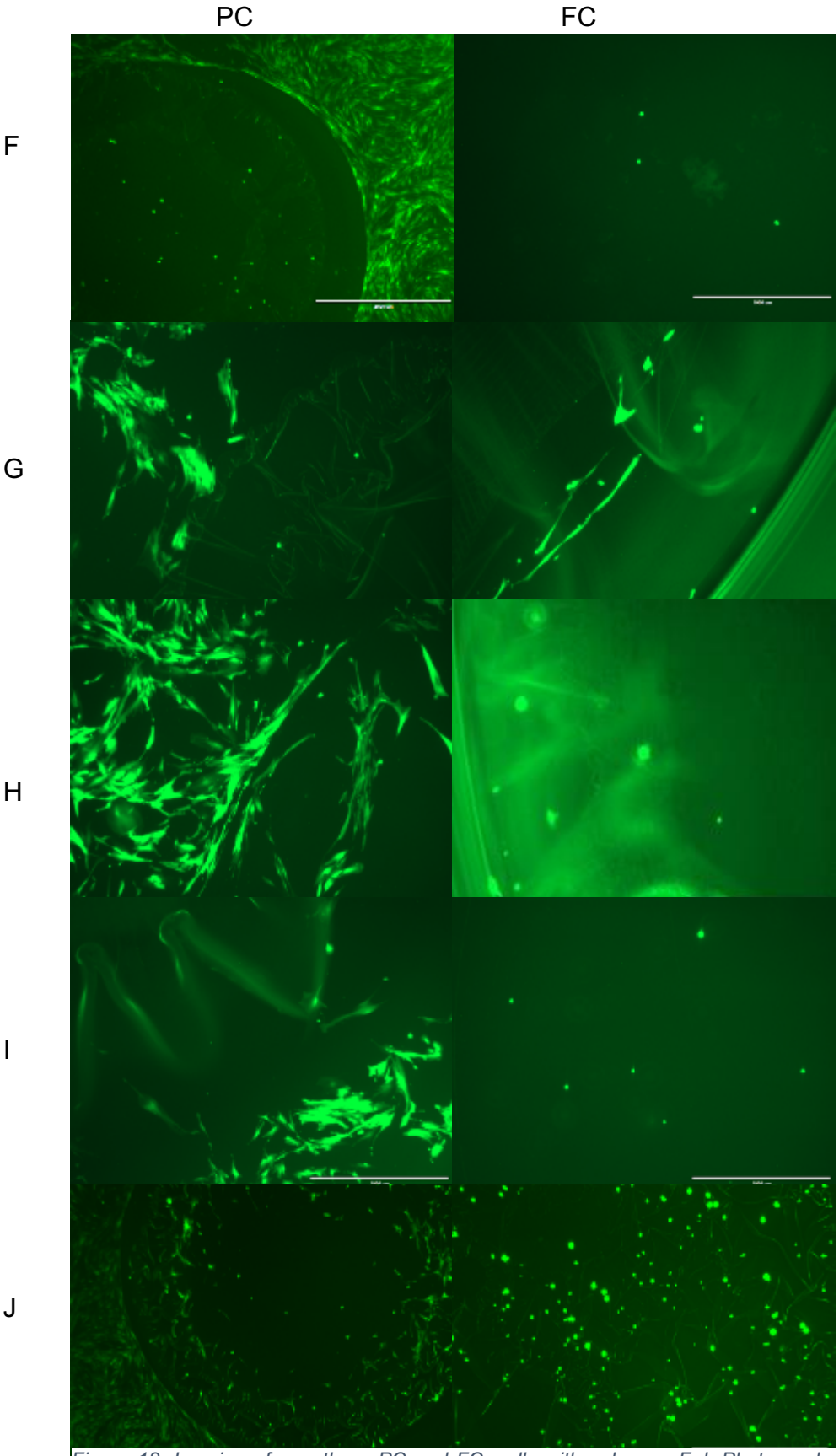

Figure 18: Imaging of growth on PC and FC wells with polymers F-J, Photography taken with EVOS in differing magnifications showing different amounts of cell growth

Polymer F: Poly[$(HEAm)_{49}$-co-$(HPAm)_{49}$-co-$(BPAm)_2$] , Side chain: hydroxyl group

Polymer F was classified as ++/+++ with little cell debris on both the PC and FC wells and a vital cell network on the PC wells.

Polymer G : Poly[$(HEAm)_{24}$-co-$(HPAm)_{74}$-co-$(BPAm)_2$] , Side chain: hydroxyl group

Polymer G was classified as +++ as there were no cells on the PC as well as on the FC wells, but also there were only a few cells on the edge with little to no network-forming indicating little growth in general.

Polymer H: Poly[$(HEAm)_{93}$-co-$(AaAm)_5$-co-$(BPAm)_2$] , Side chain: carboxyl group

Polymer H was classified as ++. There were only a few cells adherent to the outer edge of the PC wells and little to no cells on the FC wells.

Polymer I: Poly[$(HPAm)_{93}$-co-$(AaAm)_5$-co-$(BPAm)_2$] , Side Chain: Carboxyl group

Polymer I was classified as ++. Little to no adherent cells on the FC wells but also no adaquate network but differentiated cells on the edge of the PC wells.

Polymer J: Poly($HEAm_{98}$- co-$BPAm_2$) -FR, Side chain: carboxyl group

Polymer J was classified as ---. On the PC wells one can see a lot of differentiated cells which begin to form a network. The FC wells showed a lot of cell debris on the coating indicating low antiadhesive quality.

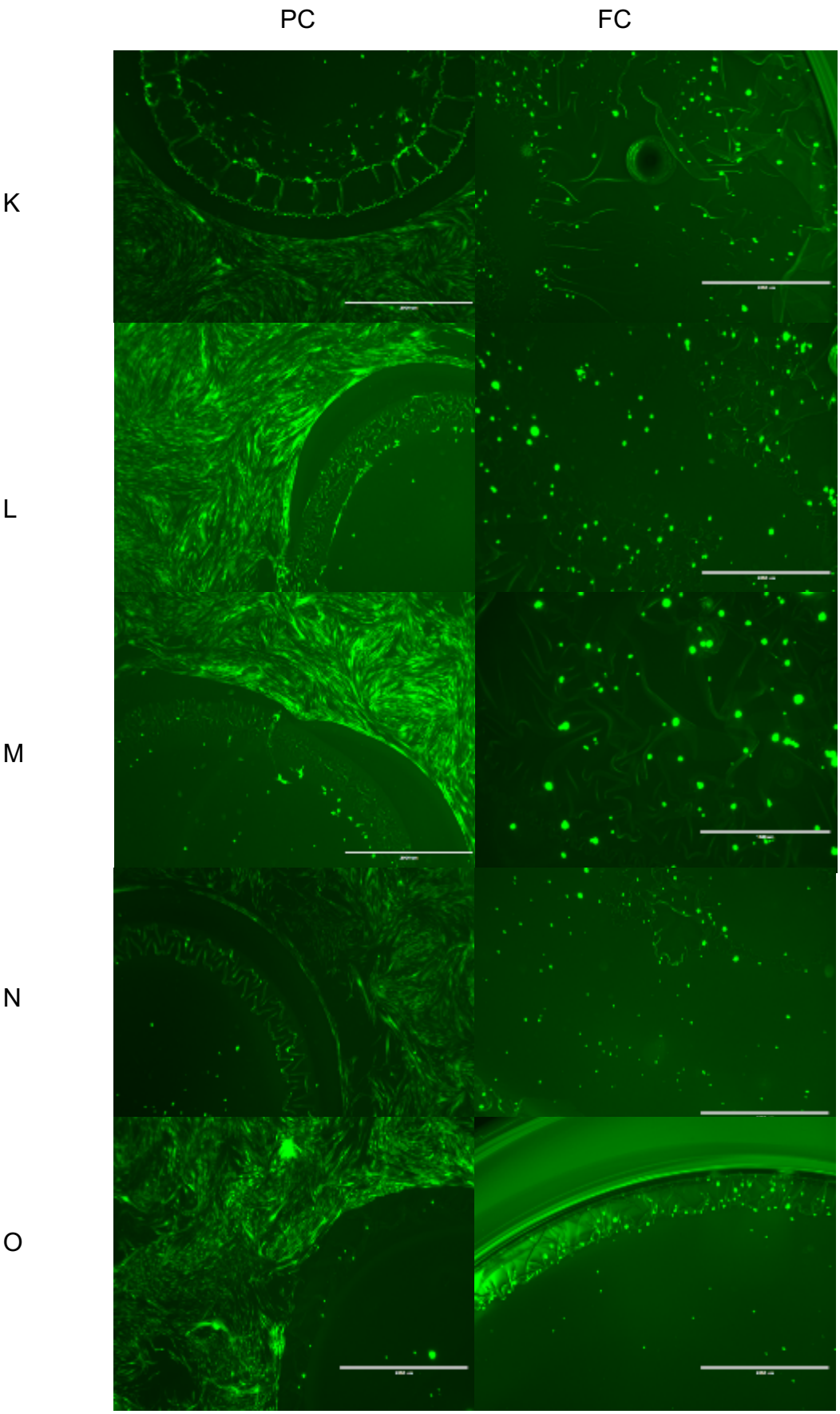

Figure 19: Imaging of growth on PC and FC wells with polymers K-O, Photography taken with EVOS in differing magnifications showing different amounts of cell growth

Polymer K: Poly(HPAm$_{98}$- co-BPAm$_2$) – free radical polymerization (FR)

Polymer K was classified as --. On the PC coated wells one could clearly see the sharp edge of the coating but also some differentiated cells on the coating. There was a network of confluent and vital cells indicating a non-cytotoxic environment but low antiadhesive quality.

Polymer L: Poly(HEAm$_{74}$-co-HPAm$_{24}$-co-BPAm$_2$) – free radical polymerization (FR)

Polymer L was classified as +++. It showed a confluent and vital cell network on the PC wells and a few non adherent, cell-debris like cells on the coating. The FC wells showed little cell debris but no differentiated cells.

Polymer M: Poly(HEAm$_{24}$-co-HPAm$_{74}$-co-BPAm$_2$) – FR

Polymer M was classified as +++. Here one could also find a vital and confluent network of differentiated cells on the edges of the PC wells indicating a good environment for cell growth but with good antiadhesive qualities of the coating. The FC wells showed little, non adherent cell debris without signs of differentiation.

Polymer N: Poly(HEAm$_{98}$- co-BPQAAm$_2$) – FR

Polymer N was classified as +++. Vital, confluent network of fibroblasts on PC wells as well as little to no cell debris on the FC wells. This indicates a good antiadhesive quality as well as a good environment for cell growth.

Polymer O: Poly (HPAM$_{98}$-co-BPQAAM$_2$) – FR

Polymer O was classified as +++. Vital, confluent network of fibroblasts on PC wells as well as little to no cell debris on the FC wells. This indicated good antiadhesive qualities as well as a good environment for cell growth.

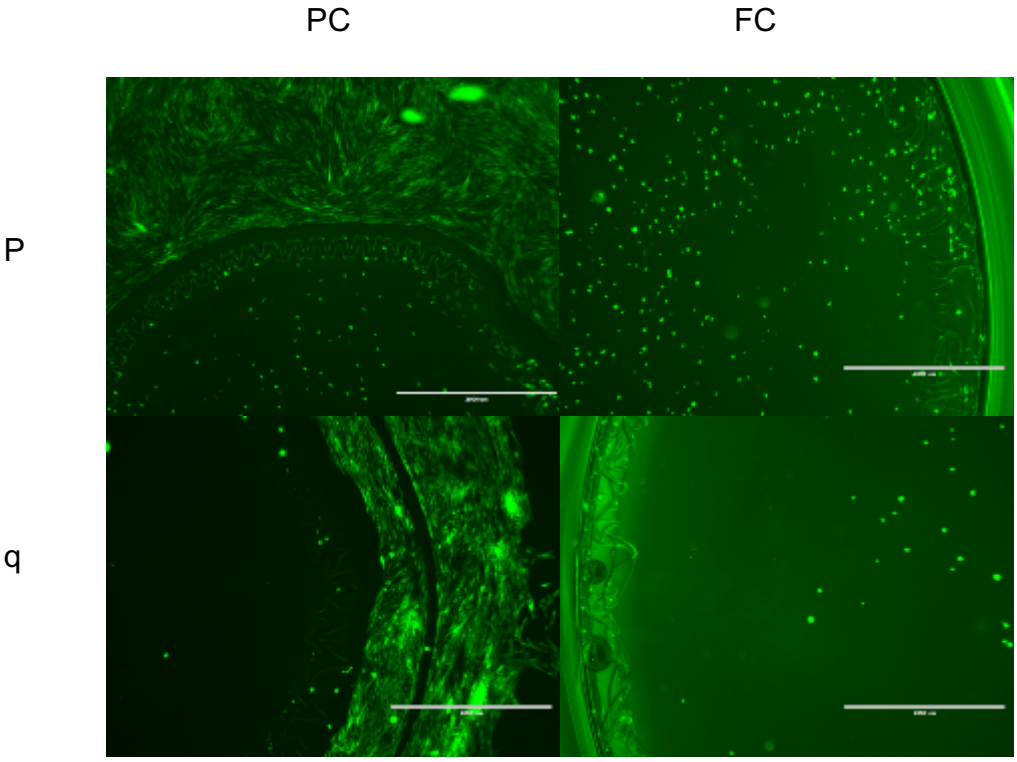

Figure 20: Imaging of growth on PC and FC wells with polymers P+q, Photography taken with EVOS in differing magnifications showing different amounts of cell growth

Polymer P: Poly($HEAm_{74}$-co-$HPAm_{24}$-co-$BPQAAm_2$) – FR

Polymer P was classified as +. On the PC well one could see a sharp edge of a confluent network with vital, differentiated cells but a lot of cell debris on the coating without differentiation. The FC wells also showed a lot of cell debris but no differentiated cells.

This indicated a non-cytotoxic environment but little to none antiadhesive quality.

Polymer q: Poly ($HEAm_{49}$-co-$HPAm_{49}$-co- $BPQAAM_2$) - FR

Polymer q was classified as ++. Little to no adherent cells on the FC wells but also no adaquate network but differentiated cells on the edge of the PC wells.

5.5.2 Tenocytes:

In the following figures, the **tenocyte** cell growth on polymer-coated plates is shown. Exemplarily for both cell types, Tenocytes 1 are shown in the following figures. All Figures show day 6/7 of growth on partially coated (PC) plates and fully coated (FC) plates. The growth was classified in the same way as previously described.

PC FC

A

B

C

D

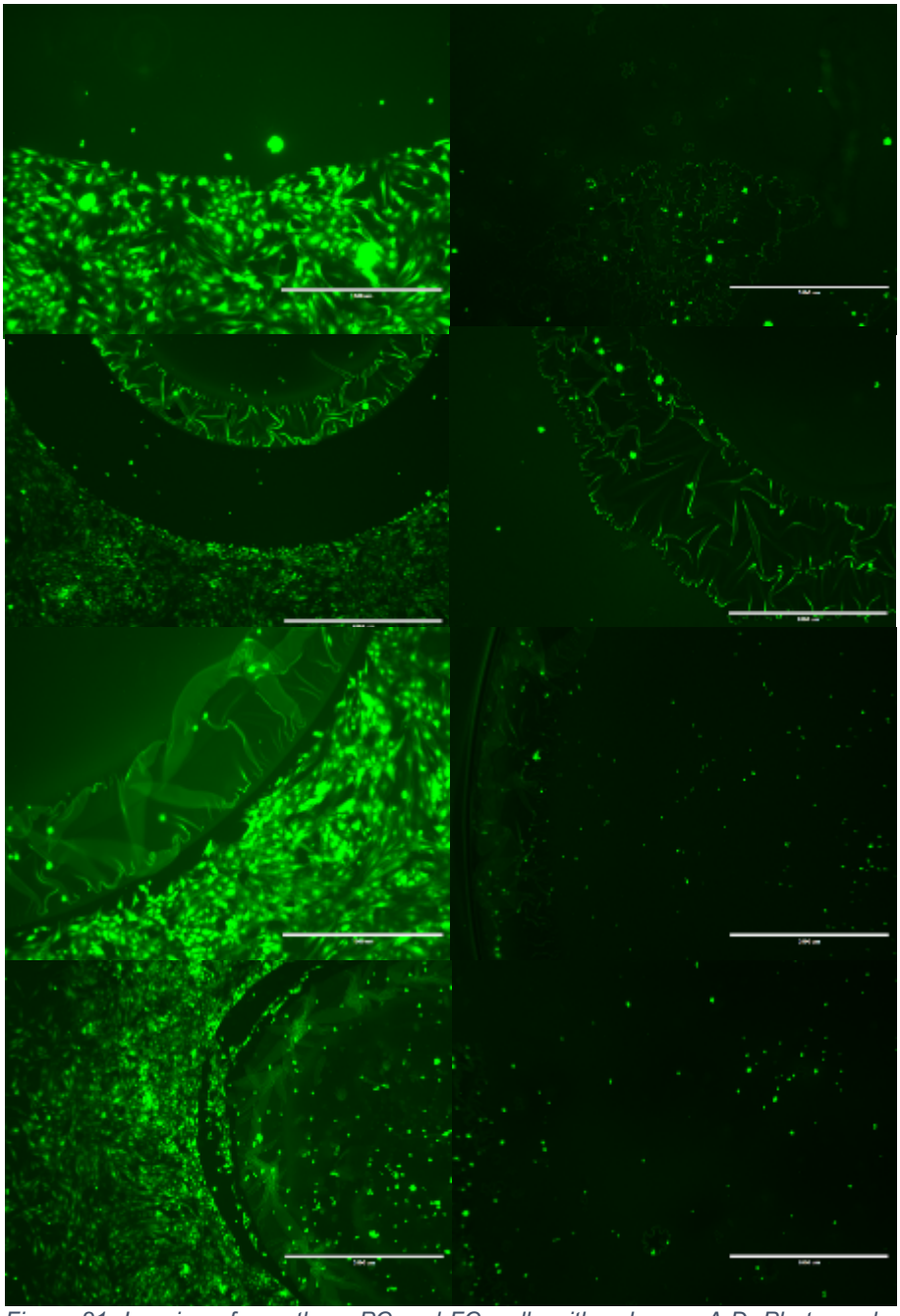

Figure 21: Imaging of growth on PC and FC wells with polymers A-D, Photography taken with EVOS in differing magnifications showing different amounts of cell growth

Polymer A: Poly[$(HEAm)_{93}$-co-$(APAm)_5$-co-$(BPAm)_2$] , Side chain: Amine group

Polymer A was classified as +++. There was a confluent network with only few non-adherent cells to the coatings.

Polymer B: Poly[$(HEAm)_{93}$-co-$(AEAm)_5$-co-$(BPAm)_2$] , Sidechain: Amine group

Polymer B was classified as ++. Vital and confluent network but some non-adherent cells/ cell debris on the coating.

Polymer C: Poly[$(HPAm)_{93}$-co-$(APAm)_5$-co-$(BPAm)_2$], Sidechain: Amine group

Polymer C was also classified as ++ with cell debris on the FC wells. There were signs of good confluent cell networks on the edge of the PC wells.

Polymer D: Poly[$(HPAm)_{93}$-co-$(AEAm)_5$-co-$(BPAm)_2$] , Side chain: Amine group

Polymer D was classified as +. There was a lot of cell debris on the coating of the PC wells without clear signs of differentiation. On the FC wells there was not that much debris and also no signs of differentiation.

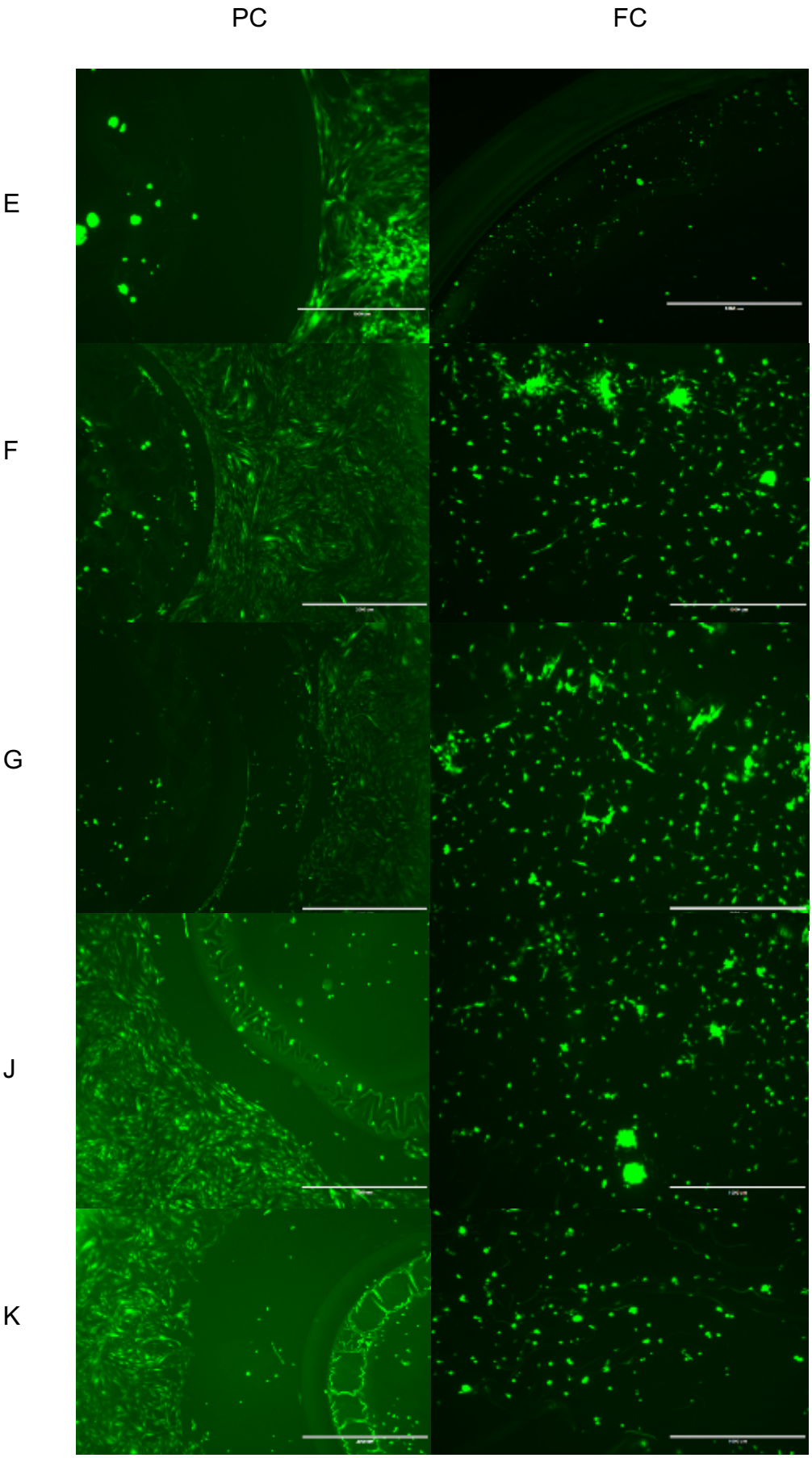

Figure 22: Imaging of growth on PC and FC wells with polymers E,F,G,J,K, Photography taken with EVOS in differing magnifications showing different amounts of cell growth

Polymer E: Poly[$(HEAm)_{74}$-co-$(HPAm)_{24}$-co-$(BPAm)_2$] , Side chain: hydroxyl group

Polymer E was classified as ++. Some cell debris on the FC wells and some on the coating of the PC wells but also a sharp edge between the coating and the confluent growth of a vital network.

Polymer F: Poly[$(HEAm)_{49}$-co-$(HPAm)_{49}$-co-$(BPAm)_2$], Side chain: hydroxyl group

Polymer F was classified as --- as one could see a lot of differentiated cells on the FC wells and the PC wells which indicates low antiadhesive quality.

Polymer G : Poly[$(HEAm)_{24}$-co-$(HPAm)_{74}$-co-$(BPAm)_2$], Side chain: hydroxyl group

Polymer G was classified as --. On the FC wells were many differentiated cells but also a lot of cell debris. The PC wells showed a confluent network with a sharp edge but also some differentiated cells on the coating.

Polymer J: Poly ($HEAm_{98}$- co-$BPAm_2$) -FR, Side chain: carboxyl group

Polymer J was classified as --- as one could see a lot of differentiated cells on the FC wells and the PC wells which indicated low antiadhesive quality.

Polymer K: Poly($HPAm_{98}$- co-$BPAm_2$) – free radical polymerization (FR)

Polymer K was classified as +. There was cell debris on the FC wells but without signs of differentiation. The PC wells also showed some debris but again no differentiation.

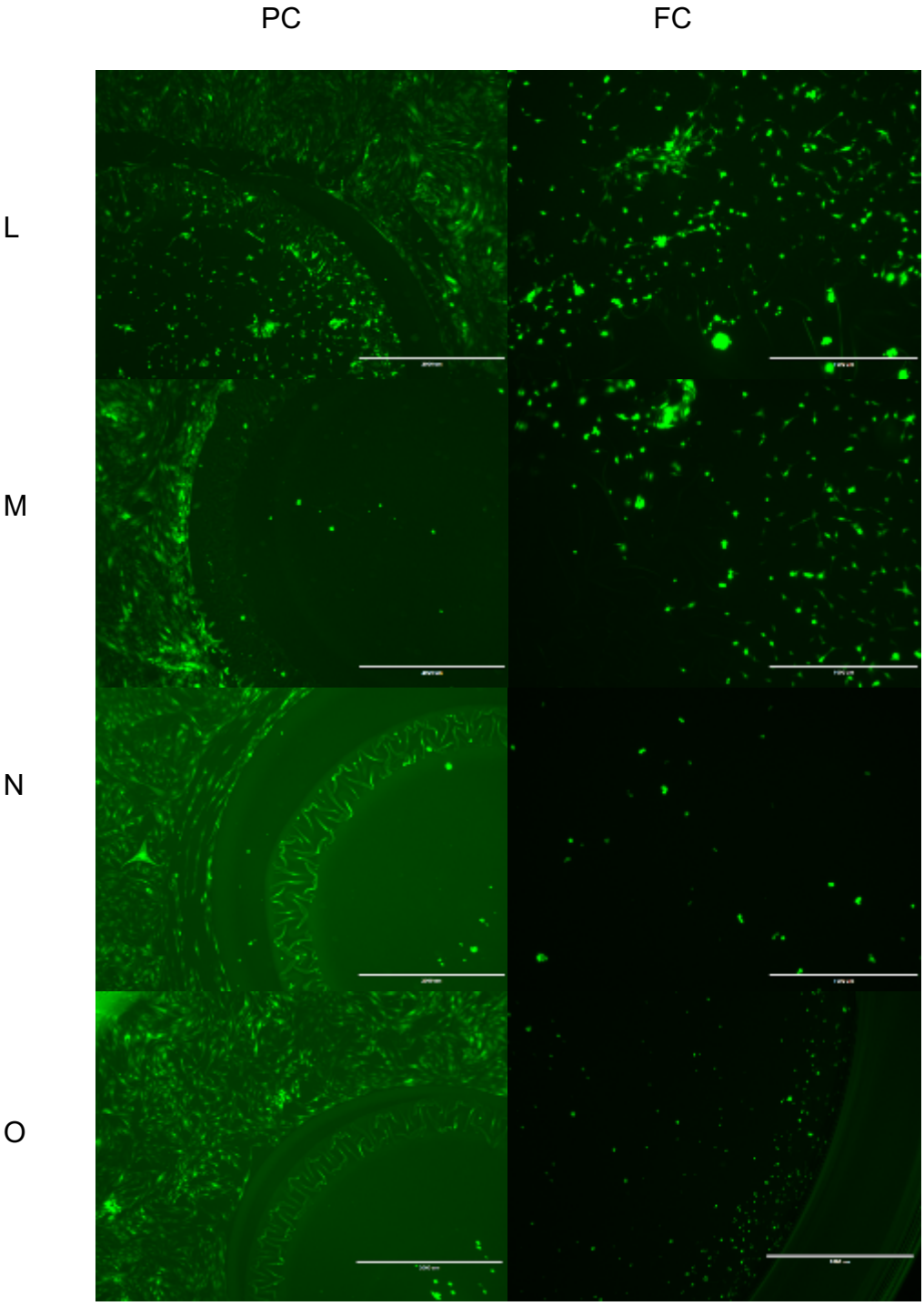

Figure 23: Imaging of growth on PC and FC wells with polymers L-O, Photography taken with EVOS in differing magnifications showing different amounts of cell growth

Polymer L: Poly ($HEAm_{74}$-co-$HPAm_{24}$-co-$BPAm_2$) – free radical polymerization (FR)

Polymer L was classified as --- as one could see a lot of differentiated cells on the FC wells and the PC wells which indicated low antiadhesive quality.

Polymer M: Poly(HEAm$_{24}$-co-HPAm$_{74}$-co-BPAm$_2$) – FR

Polymer M was classified as - - as there were a lot of differentiated cells on the FC wells. On the other hand there were little to no cells adherent on the PC wells.

Polymer N: Poly(HEAm$_{98}$- co-BPQAAm$_2$) – FR

Polymer N was classified as +++. There was a good cell network forming on the edge of the PC well but also few cell debris in the PC. The FC wells showed no differentiated cells and only little cell debris

Polymer O: Poly (HPAM$_{98}$-co-BPQAAM$_2$) – F

Polymer O was classified as ++ with a confluent network at the edges of the PC well and little to no cell debris on the FC well.

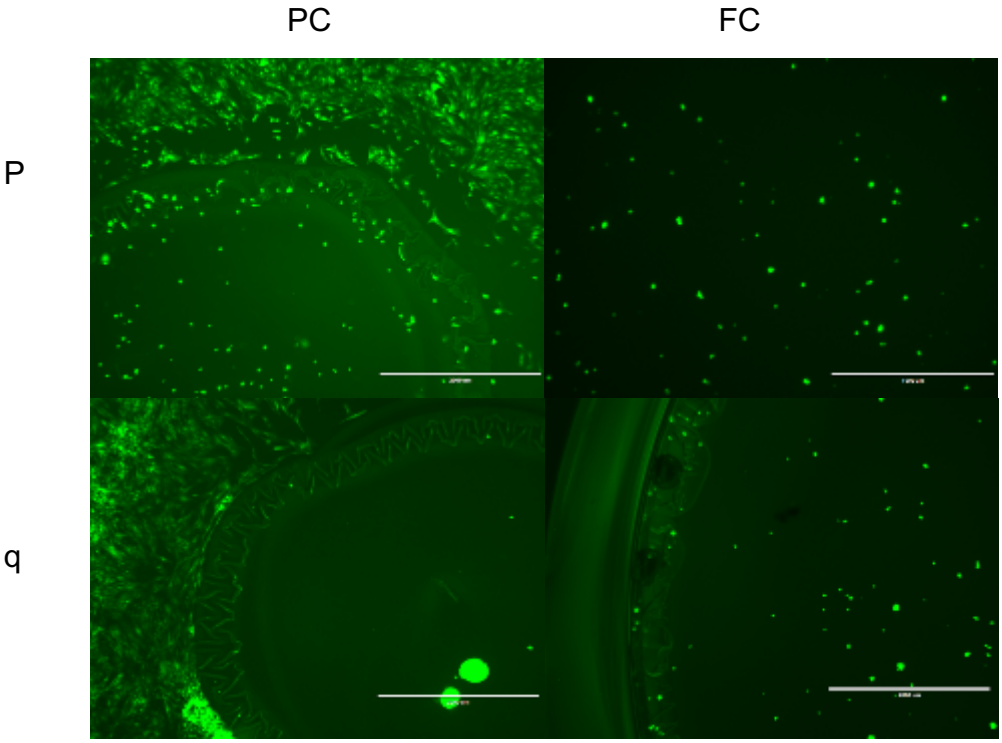

Figure 24: Imaging of growth on PC and FC wells with polymers P+q, Photography taken with EVOS in differing magnifications showing different amounts of cell growth

Polymer P: Poly(HEAm$_{74}$-co-HPAm$_{24}$-co-BPQAAm$_2$) – FR

Polymer P was classified as +. One could see a good amount of debris on the PC wells as well as on the FC wells. No signs of differentiation.

Polymer q: Poly ($HEAm_{49}$-co-$HPAm_{49}$-co- $BPQAAM_2$) - FR

Polymer q was classified as ++. There was almost no debris on the PC wells and only some none differentiated cells (debris) on the FC wells

Chart 15 gives an overview of all tested polymers and the classification of cell growth on them as well as the cytotoxicity tested with the MTT-Assay.

Coating	Cell type	Growth	Cytotoxicity	Side chain	Polymerisation	Crosslinker
A	Fibroblasts	+++	-- / 56.2%	Amine	RAFT	BPAm
A	Tenocytes	+++	-- / 56.2 %	Amine	RAFT	BPAm
B	Fibroblasts	+++	--- / 30.42%	Amine	RAFT	BPAm
B	Tenocytes	++	--- / 30.42%	Amine	RAFT	BPAm
C	Fibroblasts	++	-- /55.52%	Amine	RAFT	BPAm
C	Tenocytes	++	--/55.52%	Amine	RAFT	BPAm
D	Fibroblasts	--	---/46.25%	Amine	RAFT	BPAm
D	Tenocytes	+	---/46.25%	Amine	RAFT	BPAm
E	Fibroblasts	++ / +++	---/45.85%	Hydroxyl	RAFT	BPAm
E	Tenocytes	++	---/45.85%	Hydroxyl	RAFT	BPAm
F	Fibroblasts	++/ +++	---/29.86%	Hydroxyl	RAFT	BPAm
F	Tenocytes	---	---/29.86%	Hydroxyl	RAFT	BPAm
G	Fibroblasts	+++	---/27.97%	Hydroxyl	RAFT	BPAm
G	Tenocytes	--	---/27.97%	Hydroxyl	RAFT	BPAm
H	Fibroblasts	++	---/24.45%	Carboxyl	RAFT	BPAm
I	Fibroblasts	++	---/23.66%	Carboxyl	RAFT	BPAm
L	Fibroblasts	+++	+++/93.64%	Hydroxyl	FR	BPAm
L	Tenocytes	---	+++/93.64%	Hydroxyl	FR	BPAm
M	Fibroblasts	+++	+++/93.34%	Hydroxyl	FR	BPAm
M	Tenocytes	--	+++/93.34%	Hydroxyl	FR	BPAm
J	Fibroblasts	---	++/87.22%	Hydroxyl	FR	BPAm
J	Tenocytes	---	++/87.22%	Hydroxyl	FR	BPAm
K	Fibroblasts	--	-/77.74%	Hydroxyl	FR	BPAm
K	Tenocytes	+	-/77.74%	Hydroxyl	FR	BPAm
N	Fibroblasts	+++	+/71.12%	Hydroxyl	FR	BPQAAm
N	Tenocytes	+++	+/71.12%	Hydroxyl	FR	BPQAAm
P	Fibroblasts	+	--/55%	Hydroxyl	FR	BPQAAm
P	Tenocytes	+	--/55%	Hydroxyl	FR	BPQAAm
O	Fibroblasts	+++	--/54.72%	Hydroxyl	FR	BPQAAm
O	Tenocytes	++	--/54.72%	Hydroxyl	FR	BPQAAm
Q	Fibroblasts	++	---/39.12%	Hydroxyl	FR	BPQAAm
Q	Tenocytes	++	---/39.12%	Hydroxyl	Fr	BPQAAm

Chart 15: Overview of cytotoxicity and growth with the specific polymers on both cell types

Chart 13 highlights that there were differences in growth with fibroblasts and tenocytes. For example, polymer F was rated as ++/+++ growth for fibroblast which indicated little to no cell growth, but this seemed to have no impact on tenocyte growth as it was rated as ---.

On the other side, polymer A and polymer N were rated as +++ for both fibroblasts and tenocytes, indicating that there could be good antiadhesive properties in the tissue.

In means of cytotoxicity, we also saw large variability in the results. Some polymers seemed to create a more cytotoxic environment than others. They range from 93.64% to 23.66% compared to a native control.

In addition to the measurements of cytotoxicity it was of great interest to us how the cells would proliferate after being in contact with the polymers. The idea was that the non-adherent cells that must be suspended in the medium inside the polymer-coated well are relocated to a non-coated cell culture plate and are observed regarding their capability of growth and forming confluent cell networks.

5.6 Cell culture from seeded plates

In the following figures one can see the results of cultured cells from seeded plates at d7/d6. The cells were in contact with the polymer coatings for one day and then 500µl of medium was taken onto a fresh, non-coated well plate. 500µl of fresh medium was added. Cells were cultured like this for seven days. Medium was not changed in this time. This experiment was chosen in addition to the cytotoxicity assays to visualize growth of the cells after being in contact with potentially cytotoxic medium. Imaging was taken at day 1, day 3 and day 6 or day 7. In the following figures we chose to depict day 7 as a representative time span for growth. Exemplarily for both cell lines, tenocytes 1 are shown in the following figures.

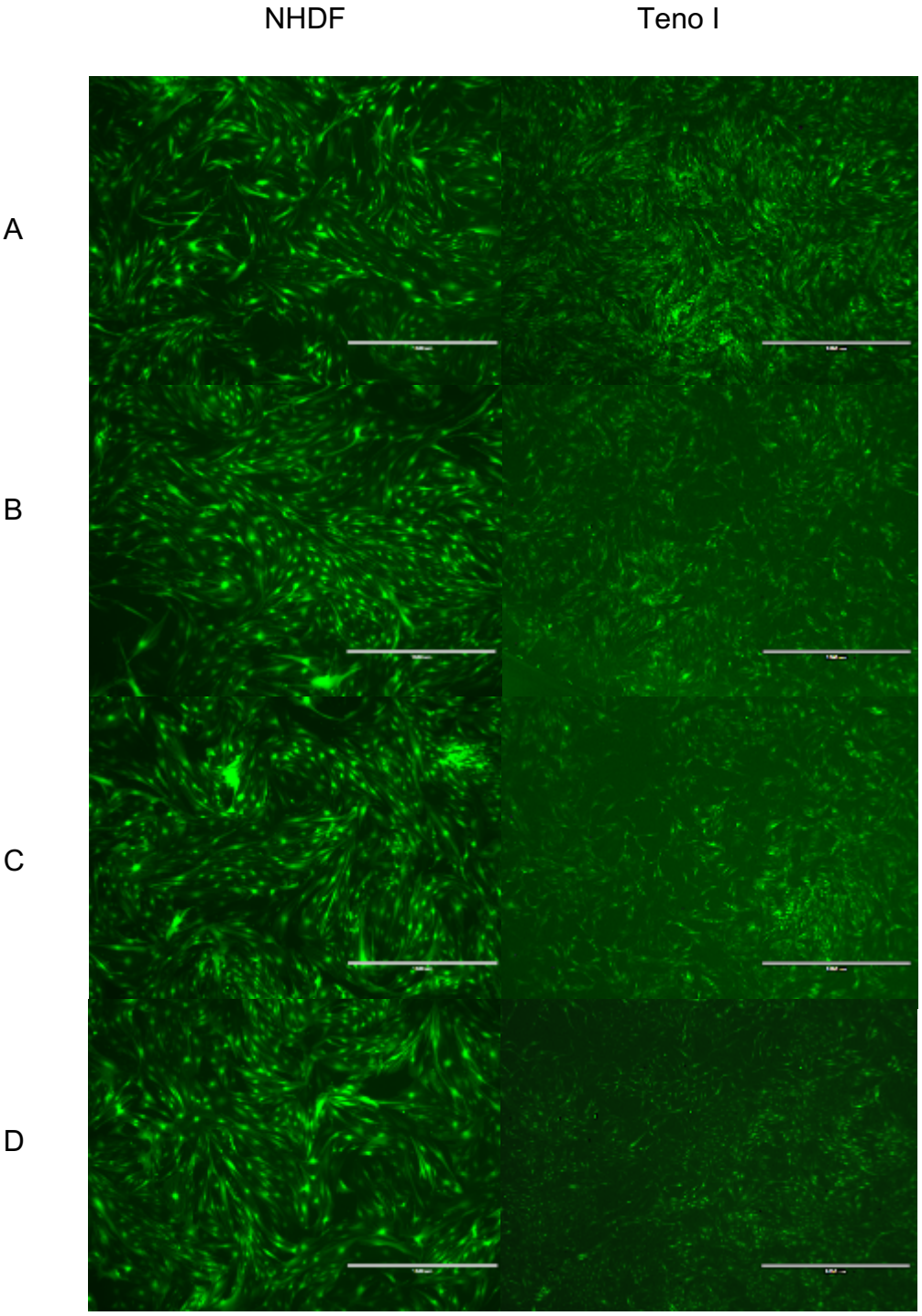

Figure 25: Imaging of cell growth after contact with polymer A-D of both fibroblasts and tenocytes, Photography taken with EVOS in differing magnifications showing different amounts of cell growth

Figure 25 shows cell growth after contact with polymers A-D. For fibroblasts one could see a good confluence after seven days as well as a satisfactory expression of eGFP of the cells. With tenocytes, one could observe largely the same results. This indicates that after being in contact with these polymers for 24h, the non-adherent cells are still capable of growth and confluence.

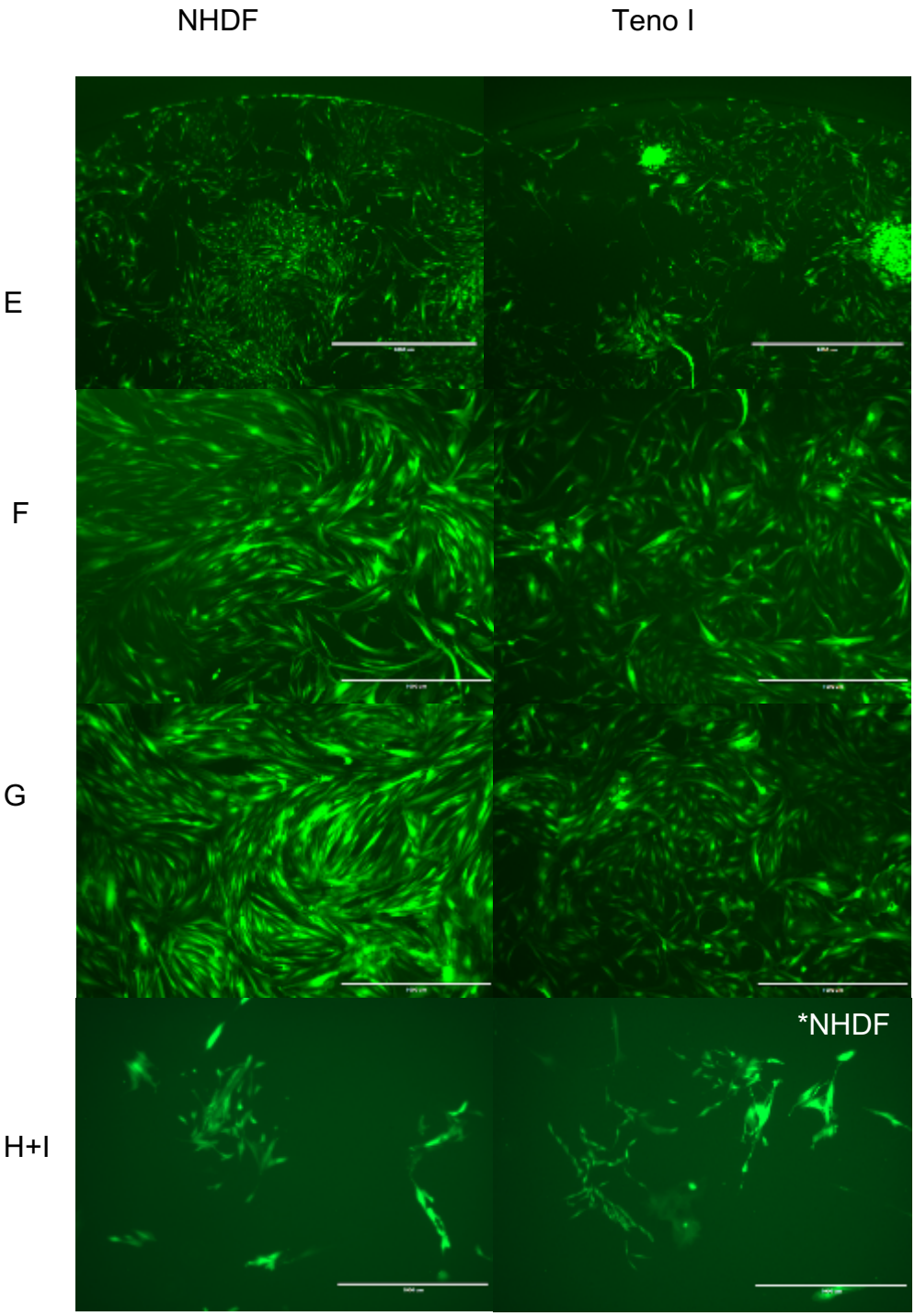

Figure 26: Imaging of cell growth after contact with polymer E, F, G, H+I of both fibroblasts and tenocytes (H+I for fibroblasts only), Photography taken with EVOS in differing magnifications showing different amounts of cell growth

In this figure the cell growth presented differently. Whereas we had good confluence and growth with F and G, there was a lack of confluence in E for both fibroblasts and tenocytes as well as a formation of cell clusters (see E/ Teno 1, figure 26). What could additionally be seen is that for H+I, fibroblast growth was lower than expected. One could see very few but differentiated cells. Cytotoxicity in the MTT assay matched this

result as it was rated --- indicating antiadhesive qualities for fibroblasts at a high level of cytotoxicity which could overall not be accepted for a later in vivo use.

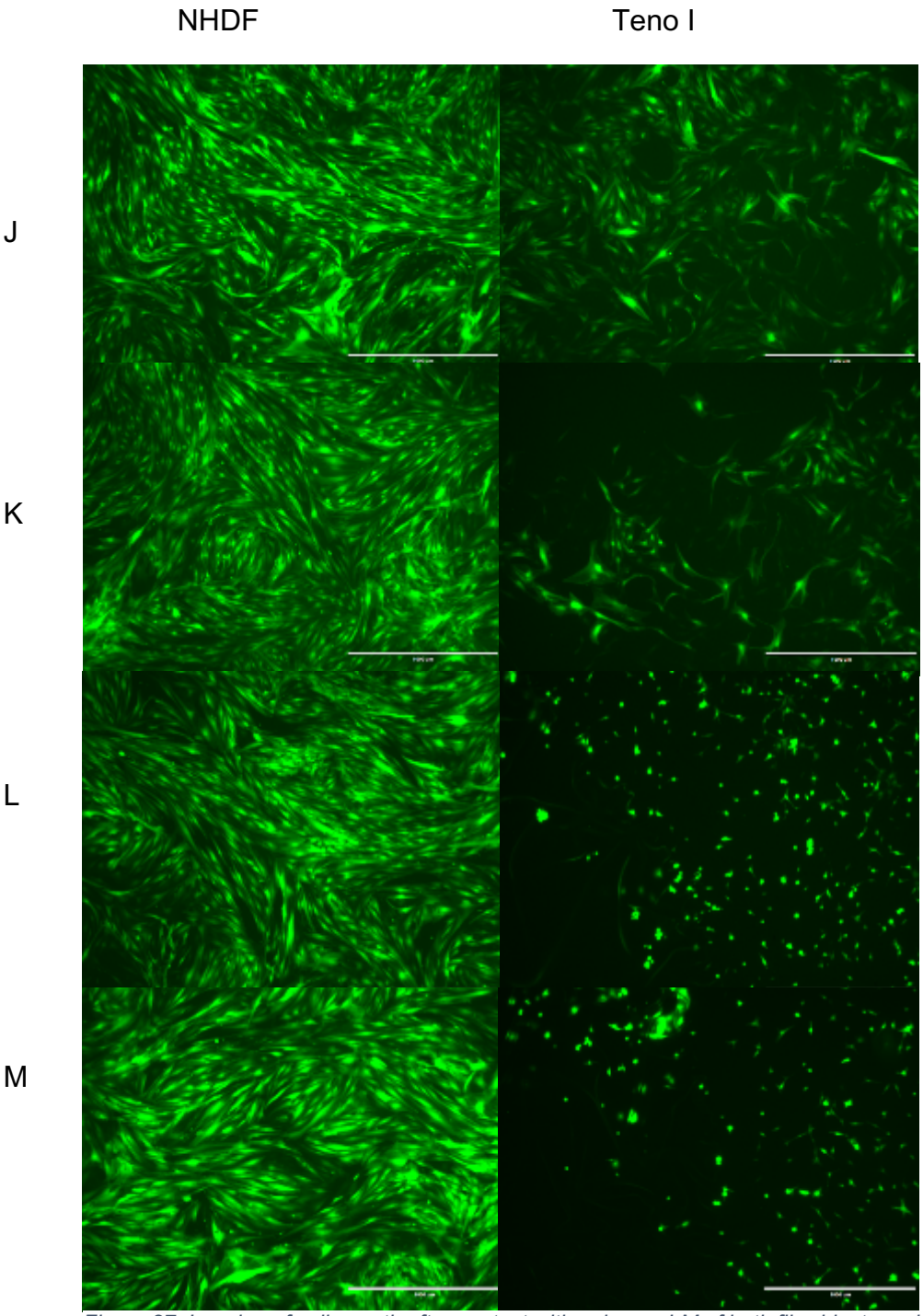

Figure 27: Imaging of cell growth after contact with polymer J-M of both fibroblasts and tenocytes, Photography taken with EVOS in differing magnifications showing different

Figure 27 shows the growth after contact with J-M. Fibroblasts showed good confluence and expression of eGFP indicating low cytotoxicity and vital non-adherent cells in the original medium. For J, tenocytes mostly presented the same whereas for K one could identify viable cells forming a network but without confluence at day 7.

With L and M there also was no confluence, and one could observe some differentiated cells but also a lot of round cells. Interestingly, cytotoxicity was rated as +++ for all the coatings above, but imaging revealed a somewhat contradictory pattern of growth for tenocytes.

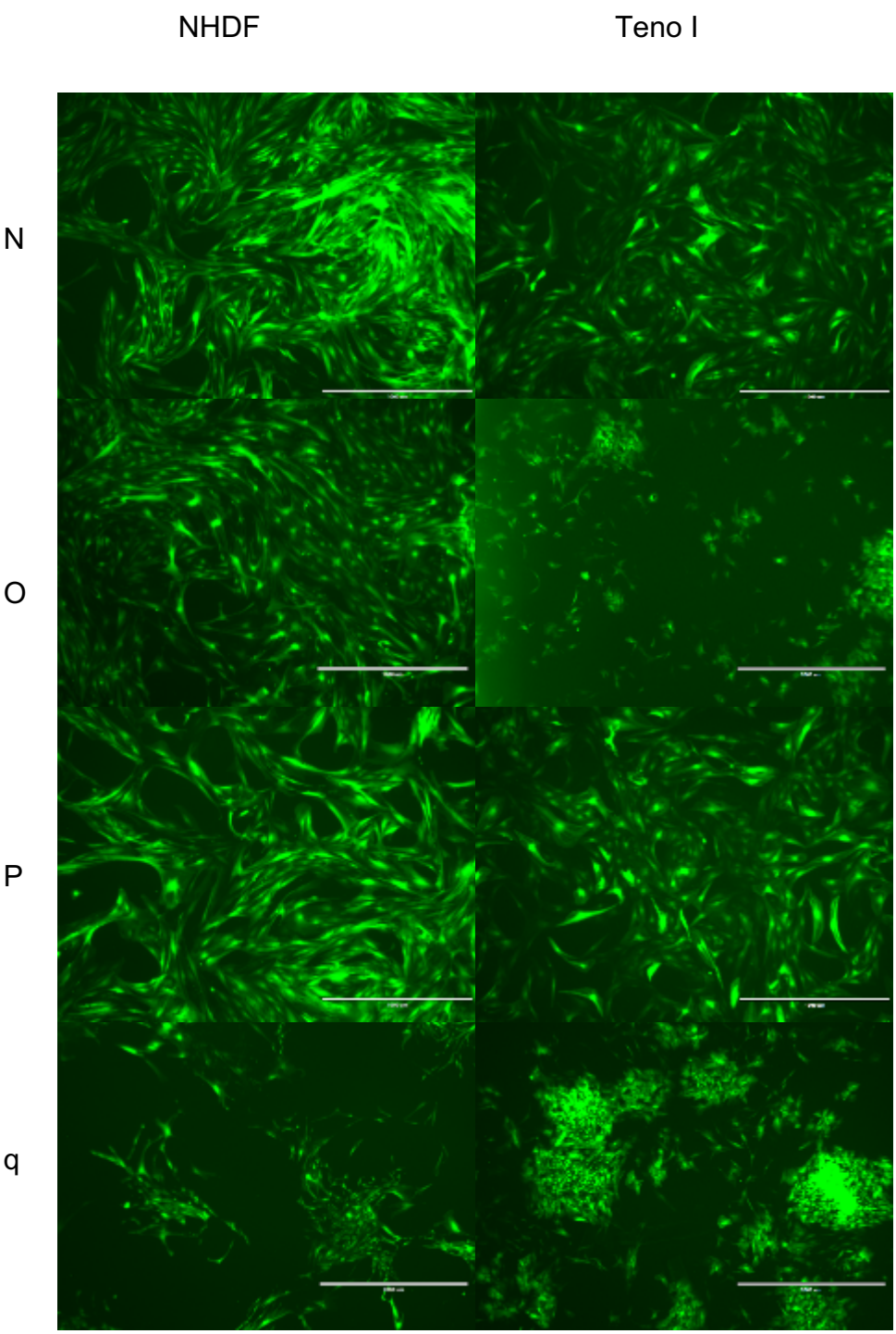

Figure 28: Imaging of cell growth after contact with polymer N-q of both fibroblasts and tenocytes, Photography taken with EVOS in differing magnifications showing different amounts of cell growth

Figure 28 shows growth after contact with N, O, P and q. With N and P, cells showed good confluence and a bright expression of the fluorescent protein for both fibroblasts and tenocytes. Fibroblasts, after contact with O also showed good confluence whereas tenocytes did not form a confluent network and tend to form cell clusters. For q, both cell types were not forming networks and tenocytes additionally formed large cell clusters with a good expression of eGFP in both. Cytotoxicity was rated as --- for q in the MTT assay which matched the observations in imaging.

5.7 RNA Isolation and RT-PCR

To further characterize the cells that derived from donor tendon tissue, we performed RT-PCR. RNA was isolated from the cells using peqGOLD Total RNA Kit. For the following PCR it was essential that the RNA sample was sufficient in concentration of nucleic acid and showed a certain purity.

RNA quality and purity was measured by using UV spectroscopy. An RNA sample of Teno 1 as well as a sample of Teno 2 was extracted. For Teno 1, the A260/A280 ratio was 1.15 and the A260/A230 ratio was 2.1. For Teno 2, the A260/A280 ratio was 1.98 and the A 260/A230 ratio was 2.07. Concentration of nucleic acid was 71.86 ng/μl for Teno 1 and 30ng/μl for Teno 2.

This indicated that there could be a contamination with proteins in sample 1 for tenocytes as the concentration of nucleic acid is high and the A260/A280 ratio is low. The A260/A230 ratio is 2.1, indicating purity regarding organic contaminants.

Sample 2 for Teno 2 is lower in concentration of nucleic acid but ratios indicate more purity regarding protein and organic contaminants.

The threshold cycle values (Ct) were calculated with the ΔCt method.

$$\Delta Ct = Ct_{target} - Ct_{reference}$$

Reference	**Hs_GAPDH**	**Hs_GAPDH**	**18S**	**18S**
Target Gene	Teno 1	Teno 2	Teno 1	Teno 2
Scleraxis	10.41	11.39	10.11	12.93
Tenascin	10.25	6.05	9.94	7.59
Tenomodulin	7.17	5.60	6.86	7.14
vWF	7.17	3.20	6.87	4.74

Chart 16: Tested reference and target genes for tenocytes with their corresponding ΔCT values

Also, a no template control was run in every cycle as a negative control. For Scleraxis and Tenascin, no Ct value was detected. Housekeeping gene 18S and Tenomodulin showed Ct values >30 and were not considered relevant. For GAPDH and vWF the Ct value of NTC was 27.32 and 25.11 which indicates contamination.

As there were signs of impurities in the UV spectroscopy for sample 1, we mainly focus on sample 2 / tenocytes 2 for evaluation.

ΔCt values show low expression for Scleraxis with a ΔCt of 11.39/12.93 and moderate expression for Tenascin (ΔCt 6.05/7.59) as well as Tenomodulin (ΔCt 5.6 / 7.14). It is observed that in these samples we measured a high expression of vWF which under normal circumstances is not expressed by tenocytes.

5.8 Microbiology

Two of the coatings were tested regarding to their antibacterial quality. Testing was performed with Staphylococcus aureus as this bacterium is known as the main cause of surgical site infections of osteosynthesis. (17) Polymer **N** was chosen as it shows intrinsic antibacterial properties, inhibiting growth of Staph. aureus in the absence of adverse side effects of classic antibiotics. Haktaniyan & Bradley outline different antimicrobial features of polymers in their review, meaning that antimicrobial effects of some polymers have been documented previously but do not describe simultaneous antiadhesive features.(79) Polymer **J** was chosen as control.

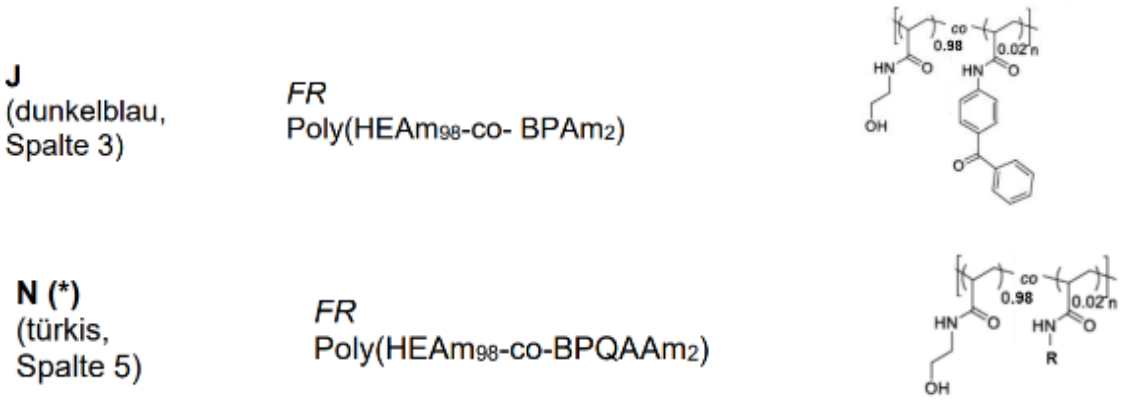

Figure 29: Polymer J and N with their structural formula which were chosen for antibacterial testing's

Petri dishes coated with polymer **N** and polymer **J** were incubated for 24h with medium that was enriched with Staphylococcus aureus. Figure 30 already shows clouding of the medium in contact with polymer **J** indicating little to no antibacterial activity. On the other hand, there were no signs of clouding with the petri dishes of polymer **N** indicating an intrinsic antibacterial activity of this polymer.

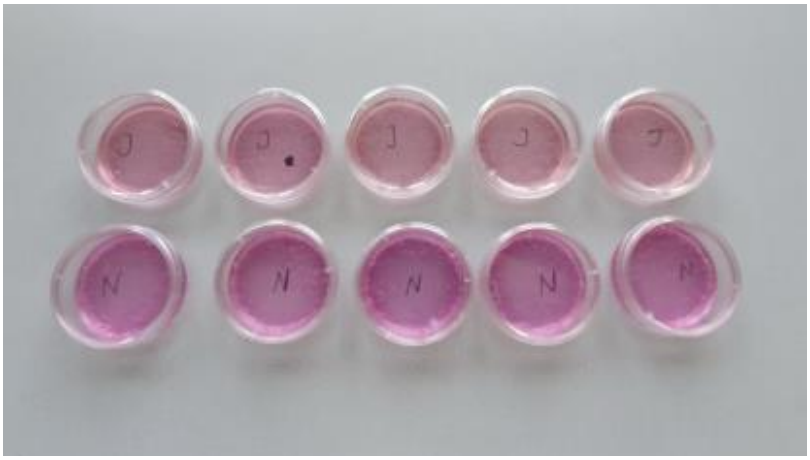

Figure 30: Polymer J and polymer N after 24h incubation with Staph. aureus

For further investigation of bacterial growth, a dilution series was set up. In A, the lowest dilution of 1:1000 of polymer **J,** one could see a vast number of colonies which become progressively fewer with increasing dilution, in D one can only see isolated colony forming units (CFU).

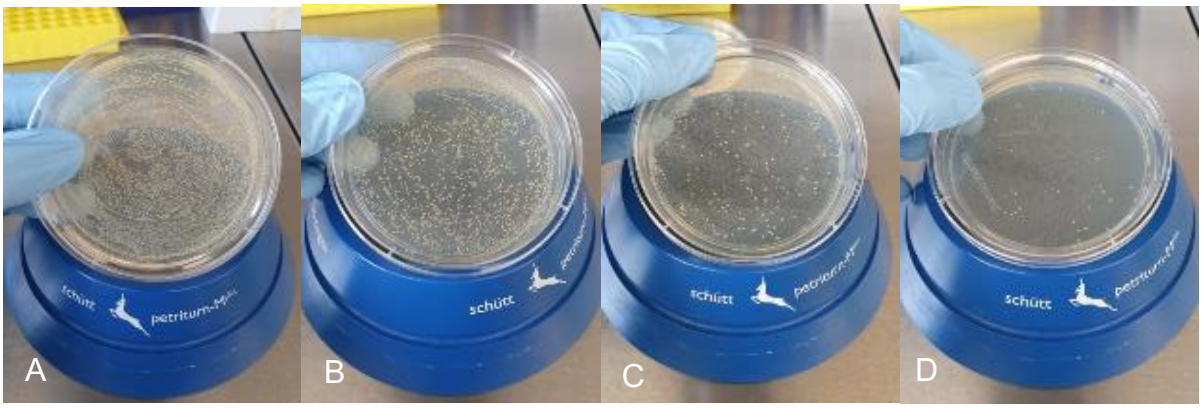

Figure 31: Dilution series of Polymer J on Müller Hinton Agar (MHA). A: Dilution 1:1000 B: 1:10.000 C: 1:100.000, D: 1:500.000 showing a decreasing amount of CFU'S with increased dilution

In contrast to this, the dilution series of polymer **N** showed no bacterial growth in any concentration of dilution. Figure 32 exemplarily shows that there was no growth in the lowest degree of dilution of 1:1000. No CFU's could be detected, indicating that polymer **N** shows clear anti-microbial effects.

Figure 32: Dilution series of polymer N on MHA. Dilution of 1:1000 showing no CFU'S indicating antibacterial properties

6 Discussion

6.1 Overview and aim of this dissertation

This dissertation investigated the impact of anti-adhesive polymer coatings on short-term medical implants like osteosyntheses. The main requirement for these polymer coatings is to inhibit adhesions in the surrounding tissue without being cytotoxic.

Seventeen polymers, all with slightly different modifications in their side chain or crosslinker, were examined regarding their anti-adhesive properties with fibroblasts and tenocytes. The main part of this work focused on the observation of cell behavior on the different polymers, reviewed microscopically after being transduced with green fluorescent protein. As a part of this work, tenocytes were isolated from donor material and were further characterized with immunohistochemistry and RT-PCR.

Like mentioned above, being non-cytotoxic was a crucial requirement for a polymer coating which is intended for a potential in vivo application in the future. Therefore, testing of the viability of cells was performed with the MTT-Assay. Also, cells that have been in contact with the medium were furthermore grown in cell culture and their behavior was observed.

Another part of this work focused on potential intrinsic antimicrobial effect of one of the polymers. Testing was performed with Staph. aureus as it is best known as the primary cause of surgical site infections of implants in osteosynthesis.(17)

In the course of this work, results indicated that some polymers seem to be preferable than others. In the following, our results regarding cytotoxicity, anti-adhesive and antimicrobial properties will be discussed.

6.2 Influence of different polymers on the adhesion process

To characterize the behavior of fibroblasts and tenocytes in contact with the different polymers, cells were seeded onto coated well-plates and cultivated for seven days at 37°C and 5% CO_2 in an incubator mimicking body temperature. Pictures were taken at day one, day three and day six or seven. No further investigation was done as there seemed to be no change in growth after this period (see figure 16). No medium change was performed during this time as we did not want to remove the non-adherent cells. Located in suspension in the medium, there could be a chance they would settle, possibly affecting the results.

However, a proportion of medium was taken off to be cultured in a separate culture to see how the cells behave after having interacted with the polymer coating for 24h. As this was done for all wells and coatings throughout this work, we did not expect the overall results to be affected by this. Cells, which were non-adherent and were suspended in the medium were not counted, so the cell count is expected to vary in cell culture because of differences in adhesion on the polymers.

To classify growth on the well plates we established a rating system based on the number of cells and their signs of differentiation. This system ranges from +++ -> --- indicating “best” and “lowest” anti-adhesive qualities. This system seemed to be most fitting to classify growth but has also shown limitations. For example, the real number of cells was not measured but they were subdivided into non-adherent cells on the coating, little and much cell debris. Debris was classified as rounded up, small cells showing no signs of differentiation like cell extensions or stages of mitosis in large magnifications under the microscope. On the other hand, “low” antiadhesive qualities were described with few, many and a lot of cells with higher grades of differentiation. This system did not allow a fluent classification of the polymers and did not represent overlapping results as some cells grew on one edge of the well but showed debris on another edge. Overall, the polymers needed to be classified to be comparable to each other which could be widely accomplished with this approach.

Pictures were taken of many perspectives and magnifications to capture the whole well to ensure adequate analysis of each polymer. Our results indicated that there were differences in the anti-adhesive properties of the polymers. Results also varied with the cell type used.

For the RAFT polymers, polymer **F** showed little to no growth with fibroblasts and was rated as ++/+++. In contrast to this, polymer **F** did not show a huge impact on tenocyte growth, mainly on the FC wells which is why this polymer was rated as ---.

Polymer **L** showed a vast amount of tenocyte growth on the PC and the FC well and was therefore rated as --- indicating very low antiadhesive properties in the context of tenocyte growth. For fibroblasts, there were hardly any cells visible on the PC wells and only few round cells on the FC well, indicating good antiadhesive properties for fibroblasts. This also was observed for polymer **M** with main growth of tenocytes on the FC wells rather than the PC wells. These two polymers derived from free radical polymerization.

In the means of anti-adhesive properties, two polymers were rated as +++ for both cell lines. Polymer **A** and polymer **N** both showed satisfactory results on the FC as well as the PC wells and therefore seemed most promising regarding the reduction of post-operative adhesion formation. Sufficient results were also found with polymer **B**, **E**, **O** and **Q**.

Polymer **H** and **I** both were only tested with fibroblasts due to the lack of polymer mass for all experiments in this work. For further studies, testing with tenocytes is needed.

These results indicated that the reduction of adhesion formation by polymers could more likely be achieved with fibroblasts than with tenocytes. Yet, two polymers showed excellent anti-adhesive properties for both cell lines and are very promising for further investigation in vivo, which will be needed.

Post-operative adhesions occur in many fields of surgery like peritoneal, pericardial or even epidural adhesions. Our main interest was to prevent postoperative adhesions of short-term implants in orthopedic surgery. Altogether, there exist many current strategies for post-operative adhesions in general.

Zhang et al. used a low-fouling zwitterionic polymer to prevent adhesion after abdominal surgery in rats. Their polymer had a viscous consistency to be able to enclose the abdominal organs. This polymer was found to prevent adhesions completely in 93% of the 42 animals tested (80). Other hydrogel-based polymers for prevention of intraabdominal adhesions are already pre-formed like Seprafilm® (Sanofi, Paris, France) (81).

To prevent tendon adhesion, Bürgisser et. al developed an elastic polymer called DegraPol. Their polymer is used as a tube around the surgical site on the tendon after surgery to prevent postoperative adhesion formation. They found, that DegraPol efficiently reduced adhesion formation of approximately 20% and even plan to load the tubes with growth factors to promote healing in future studies. (82)

Others also focused on surface modification of implants. Böker et al. used LightPLAS which is a light-based coating to change the surface of medically used steel to prevent cell adhesion. They compared the effect of the non-coated and coated steel implants on bone cell adhesion. Their results showed reduced adhesion of human osteoblast-like cells with a significant reduction of 65% in all measurements. They also measured adhesion under dynamic flow conditions in a 3D cell culture system and showed significant adhesion reduction of 56% (83).

Kuhn et al. used surface modifications by plasma-assisted deposition of hexamethyldisiloxane (HMDSO) and HMDSO with added oxygen. They found reduced adhesion and reduced proliferation of fibroblasts without significant change in the mechanical properties (84).

Our approach includes antiadhesive properties with acrylamide-based hydrogels with bezophone photocrosslinkers as well as intrinsic antibacterial qualities. Therefore, this combination of prevention of adhesion formation and antimicrobial effects presents a novel approach in surface modification and coating of short-term orthopedic implants. For a future in vivo use, further studies including animal testing must be implemented.

6.3 Cytotoxicity

It was inevitable that the polymer coatings did not show any form of cytotoxicity. As they were designed for a potential in vivo us in the future, they must remain inside the human body for the time span of fracture healing and longer until they are surgically removed. The requirement for these coatings was to act as a barrier between the short-term (titanium) implant and the surrounding tissue like tendons, periosteum and scar tissue which naturally forms after a fracture or an operation. The difficulty here is, that there is a need to create an environment on and around these coatings that is inhospitable for cells, yet without being cytotoxic. In this work, all polymer coatings used, had to be to be tested and investigated for their cytotoxic properties against surrounding tissue.

Different assays, designed to measure cell viability and proliferation are described. The principle of these assays is to visualize metabolic activity of viable cells using tetrazolium salts or resazurin. In the process of enzymatic reduction of these salts, NADH/NADPH (nicotinamide adenine dinucleotide / nicotinamide adenine dinucleotide phosphate), which are products of ongoing cellular metabolic activity, serve as co-substrates. After enzymatic reduction, a change in color can be detected and measured at its specific wavelength. The most used tetrazolium salt is MTT (3-(4,5-dimethylthiazol-2-yl)-2,5-diphenyltetrazolium bromide), yet it is not water soluble, and an additional lysis and dissolving step is essential. During this, the cells used for this assay undergo cell death. Others, like the second-generation water-soluble tetrazolium salt WST (2-(2-methoxy-4-nitrophenyl)-3-(4-nitrophenyl)-5-(2,4-disulfophenyl)-2H-tetrazolium) overcame this post-reaction process. An advantage of resazurin reduction assays is that it can be dissolved and directly used in cell cultures as they stay viable after reduction, yet it is highly dependent on temperature, pH and the initial concentration of resazurin. (85)

We used the MTT-assay, a well-established cell viability assay measuring cellular metabolic activity based on the work of Mosmann et al in 1983. (86) The MTT assay works by measuring colorimetric changes with a spectrophotometer as viable, living cells convert the MTT into formazan in an enzymatic reduction. The quantity of this change in absorbance is directly proportional to the amount of living cells. (87)

In the interpretation of our results, polymers with a rate of viability under 70% were rated as non-biocompatible, results under 40% as clearly cytotoxic. The results are interpreted in relation to a control which was set as 100%. This control were native L929 mouse fibroblasts, cultivated with medium without any form of contact with the polymers. As the results for this native control were somehow lower than the expected normal range, measurements of polymer **L** which have been comparable to a normal standard control were used as native control.

Our results showed that the polymers **A** to **I** which contained the end groups from RAFT polymerization seemed to be more cytotoxic than polymers **J** to **N**. None of these polymers showed viability over 56% indicating low biocompatibility.

Polymers **O, P** and **Q** also were more cytotoxic than **J** to **N**. Polymers **B, F, G, H, I** and **Q** were clearly cytotoxic with measurements under 40% of a normal standard control.

Best results were seen for **J, K, L M** and **N** ranging from 71% up to 94%, all derived from free radical polymerization.

In addition to the MTT measurements, a cell culture was set up where we cultivated the non-adherent cells which had been in contact with the polymers and their corresponding medium for 24h. Most results are consistent with the MTT measurements, others seem to differ. For polymers **J, K, L M** and **N** which have shown good biocompatibility, we see excellent growth for fibroblasts, tenocytes show this only for **J** and **N. H** and **I** have only been tested with fibroblasts, yet we can observe less growth without any signs of confluence. These were also rated clearly cytotoxic with MTT. **Q** showed inadequate growth for both tenocytes and fibroblasts in agreement with cytotoxicity assays. Interestingly, **O** and **P** showed adequate growth and confluence for fibroblasts, **P** also for tenocytes.

Regarding these findings, fibroblasts appear to be somewhat more resistant to the polymer coatings than tenocytes. However, this cell culture also showed us that there was visible growth of fluorescent cells after contact with **all**, even clearly cytotoxic polymers. Sometimes, cell clusters were visible. Whether they formed as a sign of stress-reaction to the environment remains unclear. Cultivation of cells over a longer period could be interesting, as to see if the cells can still regenerate afterwards and form a confluent, viable network.

However, these results indicated differences in cytotoxicity regarding the origin of cells and the results of cytotoxicity assay should always be carefully evaluated.

Ghasemi et al. have investigated the utility, limitations and pitfalls of the MTT-Assay that need to be taken into consideration when interpreting the results. They evaluated potential confounders like MTT concentration, incubation time, serum starvation, media composites, number of seeded cells etc. with a prostate-cell cancer line. They found that an increase in seeded cells elevated the levels of formazan produced by measuring the optic density. Also, without any change in concentration of MTT or an increased number of cells, an increase in incubation time led to a higher optic density with a plateau after 3h with 20.000 cells and a concentration of 0.3 and 0.4mg/ml of MTT. With lower cell numbers, it took up to 4h of incubation, indicating that the number of cells and concentration of MTT affected the reduction process. Additionally, they found that an increase in MTT concentration from 0.4 mg /ml to 0.5mg/ml did not affect optic density. They explain this to themselves as an acceleration of cell death at higher levels of concentration of MTT. Media components could also affect the optic density so they recommend replacing the media with serum-free media previously to the assay to avoid measurement-errors as fetal calf serum can cause minimal rise in optic density levels. What seemed important, was the fact that cells which showed apoptotic features still can reduce MTT to formazan. They implicated that morphological studies of cells are needed in addition to this assay. (88)

The MTT-Assay is a valuable, well-established assay to measure cell viability. One must know that this assay leads to cell death, so it is designed for end-point measurements only, rather than a viable cell culture. Our results clearly rated some polymers as cytotoxic, excluding them from any further investigations for in vivo use. A biocompatibility of over 70% was reached for several polymers giving a promising outlook for further research.

6.4 Isolation of tenocytes

Part of this work was the isolation of tendon cells (tenocytes) from donor material. Consent of each patient was present as well as an agreement between the Ethics Commission of the State Medical Association of Mainz and the University Medical Center regarding donor material in research.

Donor material is a crucial part of medical research to extract human cells to work with. The prerequisite must be that these materials are otherwise medical waste and are not needed to be sent to pathology.

We needed several attempts to isolate the cells from donor material. In all trials, tendons were washed thoroughly with PBS and cleaned from excess tissue like muscle cells and adipose tissue ensuring that no other cells would be cultivated. For the first attempts, tendon cell isolation was tried to be achieved by enzymatic digestion with 0.2% collagenase I in the medium (DMEM/ F-12 + GlutaMax (Gibco®, Life Technologies, Grand Island, NY, USA) + 10% FCS (Biochrom AG, Berlin, Germany) and 1% Penicillin/Streptomycin (Sigma-Aldrich, St. Louis, US)). In a second attempt, concentration of collagenase I was set to 0.5% and was incubated on a rotating plate.

We could finally achieve isolation of tenocytes by adding ascorbic acid to the medium and incubating the tendon fragments in a 6-well plate for several days, without any enzymatic digestion at all. Two cell lines were obtained, called Teno 1 and Teno 2.

For further investigation of these cells, immunohistochemistry and RT-PCR was performed.

Immunohistochemistry:

We chose Calponin 1 and Tenomodulin as markers for immunohistochemistry. Calponin 1 acted as a marker for smooth muscle cells and interacts with α-Actinin-Actin. (78) It is not seen as a marker for tendon cells in general but is limited to detecting vascular structures in tendons.

Tenomodulin is a transmembrane glycoprotein, expressed in dense connective tissue such as ligaments and tendons. (53)

The results of immunohistochemistry showed excellent expression of both markers in cell lines Teno 1 and Teno 2. Especially the expression of tenomodulin, which served as a very specific marker for tenocytes indicated and highlighted that these cells derived from tendons. Cells also were stained with Hoechst dye to visualize nuclei.

In another experiment, we immunohistochemically stained both markers (CNN1 and anti-TNMD) at the same time. This experiment also served as a control but again underlined the origin of these cells to be most likely tendon derived cells.

RT-PCR:

To further characterize the tendon-derived cell lines, we used RT-PCR. As a first step, RNA was isolated from the cells.

For Teno 1, RNA quality and purity could not be reached sufficiently, Teno 2 showed adequate measurements. PCR was performed with both cell lines for Scleraxis, Tenascin and Tenomodulin as specific markers for tendon cells. Van Willebrand Factor was also added as a marker for vascular endothelial cells and served as a control. Results for both cell lines are presented in chart 16 with focus on Teno 2 because of the quality of the RNA sample. GAPDH and 18S served as markers for housekeeping genes as reference.

We observed a low expression of Scleraxis with a ΔCt value of 11.39/12.93. This expression was not considered relevant. Tenascin and Tenomodulin both were expressed with ΔCt values with a range of 5.6 to 7.6 showing a moderate expression in these cells. What was not expected was the high expression of vWF with ΔCt values of 3.2/4.7. vWF served as a marker for vascular endothelial cells and should not be expressed in tendon cells. Given the results of the immunohistochemistry, with a clear detection of tendon-cell specific marker tenomodulin, it is unlikely that the given cell line is of vascular origin. The fact that Scleraxis could not be detected in RT-PCR has already been previously reported. (66)

Han, W. et al. described that with increasing age of the donors, tendon stem/ progenitor cells showed an upregulation of the senescence marker p16 as well as SA-β -gal (senescence-associated β-galactosidase) and therefore a decrease in the expression

of the following tendon-associated markers: tenomodulin, scleraxis, biglycan, decorin, Collagenase I and III. (89)

These results indicated that the characterization of tenocytes can vary, depending on the age or passaging of the isolated cells. Knowledge of the age of the donor or the passage is helpful for choosing the right markers.

In literature, different approaches for tenocyte isolation have been described.

Han, S. et al. attempted to isolate degenerative tendon cells in patients with tendinopathy, so they harvested the extensor carpi radialis brevis tendon from patients with epicondylitis. Their protocol focused on enzymatic extraction with collagenase II and tenocyte origin was confirmed with immunohistochemistry with the detection of tenomodulin and mohawk as representative markers of tenocytes (90).

Research of Wagenhäuser et al. concentrated on isolating tenocytes for tendon tissue engineering of rotator cuff tears. They isolated tenocytes from the long head of the biceps tendon from patients receiving shoulder arthroplasty using two different methods for isolation: enzymatic extraction with 0.2% collagenase I and cell migration of tendon cells from the tendon fragments in medium. Ascorbic acid was also added to their medium. To confirm the origin of their isolated cells, they performed RT-PCR. Tenascin and Scleraxis were found for both cell lines in both extraction methods. Interestingly, the expression of tenomodulin could not be detected in their cells. They explained this phenomenon as a loss of this marker during passaging. They stated that both methods showed equal results in the isolation of tenocytes, with the advantage of shorter timespan between harvesting the tendon and cell seeding with the enzymatic extraction (89).

Isolation of tenocytes can be obtained in different ways, either enzymatic or through cell migration from the donor material. Both ways seem to be equal regarding current literature. Characterization with RT-PCR and immunohistochemistry also is an important part to verify tendon-origin but donor age and cell passage must be considered.

6.5 Antimicrobial effects

In addition to the antiadhesive effects of the polymers we studied in this work, we also examined the intrinsic antibacterial effect of polymer **N** and polymer **J**.

The idea of an antibacterial coating of short-term as well as long term implants especially in orthopedics like endoprosthesis is not new altogether. Many strategies for infection prevention have been described in literature. Focus of research lies on surface modifications, coatings that release antibiotics or antibacterial substances. The main point is to maintain a non-cytotoxic yet antibacterial environment in vivo for the surrounding tissue. On the other hand, complications like antibiotic-resistant bacteria and the formation of a biofilm remain a challenge.

Implant infection being a huge problem, device associated infections accounted for 25.6% of all healthcare-associated infections in a study of Magill et al. in a multistate prevalence survey in 2011. (91)

Staphylococcus aureus, being the bacterium which is mainly responsible for surgical-site infections of osteosynthesis was chosen for this testing. (17) A dilution of Staph. aureus was applied to polymer-coated petri dishes. After cultivation for 24h, we observed clouding in the petri dishes with polymer **J**. The petri dishes with polymer **N** did not show any signs of clouding at all, underlining the expected anti-microbial effect of this polymer. For further confirmation of these observations, the suspension was plated on Müller Hinton agar plates with a Drigalski spatula in a dilution series and CFU's were analyzed.

All plates with the suspension in contact with polymer **J** showed bacterial growth, decreasing with increased dilution. However, all agar plates which have been plated with the suspension in contact with polymer **N** did not show any signs of bacterial growth, not even in the lowest dilution of 1:1000. This shows the clear antibacterial effects of polymer **N** with Staph. aureus.

Numerous studies exist, concerning anti-bacterial coatings, surface modifications, antibiotic-releasing coatings or implants like antibiotic-loaded bone cement. One must differentiate between short-term implants, only remaining until fracture healing is achieved in contrast to long-term implants like hip or knee arthroplasty implants, designed to last over many years.

Implant-associated infections tend to follow a foreign body reaction, as granulation tissue forms at the infection site, combined with a fibrous encapsulation. (92) What results, is a predisposition for the formation of a biofilm and bacterial adhesion. Biofilms are produced by the formation of microcolonies of pathogens producing a protecting layer, helping them to survive in the host. (93)

Chen et al. gave an overview of current strategies of antibacterial coatings on orthopedic implants in their review in 2023. They stated that there exist three main approaches of antibacterial coatings: anti-adhesion, contact-killing and the releasing type. (94, 95)

Adhesion-resistant coatings work by limiting or eliminating bacterial adhesion to the implant and consequently preventing biofilm formation. (96) Zwitterionic polymers, hyaluronic acid, sodium alginate, polyethylene glycol are all hydrophilic polymers which can be used as coatings with a good effect against bacterial adhesion. (97, 98) In contrast to the hydrophilic coatings listed above, hydrophobic coatings have also been investigated but further studies especially in vivo are needed to implement them in clinical practice. (99)

Coatings with active, antibacterial substances fall under the category of contact-killing antibacterial coatings. There are different antibacterial agents used with this method. Antibiotics, antimicrobial peptides, metals like silver or copper, enzymes, organic cationic compounds like chlorhexidine or chitosan, organic non-cationic compounds and other non-organic compounds like nitric oxide or TiO_2 and TiO_2 based nanocomposites are listed as the main antibacterial compounds for contact-killing coatings by Cloutier et al. (100)

The releasing-type antibacterial coatings work by releasing the antibacterial substance from the coating. Antibiotics being released from implants have been of great importance especially in the field of orthopedic surgery. E.g. the use of antibiotic-loaded bone cement which can be mixed with different antibiotics is studied by various groups. (101)

To summarize their review, Chen et al. stated, that it is advisable to combine two or three antibacterial coating mechanisms to prevent surgical site infection and formation of biofilm. Yet, they also highlight the remaining challenges of this field like maintaining a long-lasting antibacterial activity, stability of the coatings and their safety. (94)

Although there has been a lot of research with very promising outcomes, there is still a gap to clinical use of antibacterial coatings for implants.

Our polymer **N** provides intrinsic antibacterial effects without the side effects of antibiotics like resistances and without cytotoxicity. This polymer combines antiadhesive as well as antimicrobial properties and serves as a novel approach for the coating of short-term implants in orthopedic surgery. Further studies of this polymer including in vivo studies will be needed but the in vitro results give a promising outlook to the future.

6.6 Strengths and Limitations

In the following part the strengths and limitations of this study will be discussed.

A strength of this study is its high relevance for fundamental research and clinical use as the need for antiadhesive and antibacterial implants rises with increased medical opportunities. Implant removal is one of the most frequent orthopedic surgeries. A demographic study of orthopedic patients before and during the COVID-19 pandemic showed that in 2020, 30.5% of all orthopedic surgeries were implant removals. (3) This underlines the clinical importance of implant research to prevent risks like nerve injury, refracture or infection with removal. (102) With that being said, we must mention a limitation of our study as this is an in vitro study only. Conclusions for an in vivo use cannot be drawn without further investigations as the behavior of cells in culture may not fully reflect the cells behavior in tissue.

We used different methods to validate the cells behavior on the coatings, particularly in the question of cell viability. Cytotoxicity was measured with a functional, well-established assay (MTT-Assay, DIN ISO 10993-5) and was combined with imaging on the coatings in a separate culture. This presents another strength of this dissertation.

Imaging of growth on coating was performed regularly on d1, d3 and d7. For further studies, the period of observation could be prolonged. Our imaging ended at day 7, but it could be interesting to study the cells behavior on the coatings over a longer period as implants need to stay in place for the time of fracture healing. However, the translatability to in vivo growth is hard to draw at this point.

Two polymer coatings, **H** and **I** have not been tested with tenocytes. For the repetition of MTT's and fibroblast cultivation, polymer mass was not enough, so we can only rely on the results of fibroblast seeding for these two polymers. As cytotoxicity for both polymers was <25% compared to control, these two did not reach compatibility for any in vivo use and will therefore be excluded for further investigations and experiments anyway.

Additionally, antimicrobial activity of polymer **N** was studied and showed clear-antibacterial effects against Staph. aureus. This combines anti-adhesive and anti-bacterial properties for this polymer and is a definite strength of this work as it presents a promising outlook to further in vitro studies.

Also, part of the cells used in this work were isolated from donor material and having used two different cell lines for our study is not found with many others. On the other side, cell characterization could have been further investigated by testing more tendon-specific markers. PCR could have been repeated as well as RNA-Isolation to generate better quality of the samples to rule out impurities for the further measurements.

Yet, cell characterization was again studied with different methods as we immunohistochemically tried to confirm the cells origin as tenocytes and combined this with RT-PCR. We see this combination of methods clearly as a strength to this work as we can interpret the detection of tendon specific markers in different ways.

To conclude all the points mentioned above, this study represents an approach in fundamental research of short-term implants in orthopedic surgery. Further investigations of polymers regarding their anti-adhesive properties need to be added but it provides a promising outlook in the field of anti-adhesive and at the same time anti-microbial implants based on this dissertation.

6.7 Future directions

We see the main field of application for this anti-adhesive and anti-microbial polymer-coatings in the treatment of fractures with short-term implants. Those implants, mainly consisting of titan are used in treatment of displaced fractures with a need of operative therapy. Consecutively, tissue damage occurs with these injuries. As these implants, especially in hand surgery are anatomically close to tendons and ligaments, scar tissue forms with the risk of postoperative adhesions, impacting mobility and resulting in pain as well as the risks which come with implant removal.

As these results derived from in vitro experiments and studies, it is essential to know that these cannot be transferred in vivo altogether so further studies regarding this field will be needed. We must investigate the behavior of the polymers on titan and following this, the behavior and growth of cells on coated titanium in vitro.

It is also important to keep in mind, that during operation, these coated plates will undergo mechanical stress. Plates need to be bend and repositioned multiple times to create optimal fracture reduction. Polymers need to be firmly attached to the titanium without any signs of detachment. Blood, fat and lymph create a unique environment in vivo during the healing process. Additionally, biocompatibility of a coating is a must, as we do not want to risk a foreign body reaction.

With Polymer N, we have a polymer that inhibits intrinsic antibacterial activity against Staph. aureus. It needs further microbiological testing to gain knowledge of its antibacterial activity against other bacterial species like e.g. Staphylococcus epidermidis which is also a relevant cause of surgical site infection. (103)

When all in vitro studies are done, the first in vivo studies need to take place, possibly with small animals like rats or mice. Of course, this must be carried out under ethically appropriate conditions, but it is important to study the formation of adhesions in an in vivo model.

All in all, there are very promising outlooks to the future based on our current results with a long way to go until these polymers are ready for application in the human body.

7 Conclusion

The treatment of fractures with implants is a tremendous part of orthopedic surgery. If these implants do not cause any sort of problems, they can remain in the body without a need of removal. Nonetheless, there are some indications for implant removal, explicitly infection. However, implants in the joint area or those which interfere with mobilization should be removed. Above all, the patient's desire for implant removal remains central to the decision-making process. Especially in areas of the body where tendons are near the fracture e.g. in palmar plate osteosynthesis of distal radial fractures, erosions of the flexor tendons after implant removal have previously been described. (2) These procedures account for a large proportion of all orthopedic operations (30.5% in 2020 in Germany (3)) and are associated with non-negligible risks like persistent pain and refractures. (4)

We have addressed this underlying clinical problem and have tested polymer-based coatings regarding their antiadhesive properties. Human fibroblasts and self-isolated tenocytes from donor material were seeded on these coatings in vitro. These were examined immunohistochemically and via RT-PCR and analyzed for their specific markers. To visualize the cells on the coatings, they were transduced with green fluorescent protein by using a lentiviral vector system. Polymer **N** and **J** also were investigated regarding antibacterial properties where polymer **N** showed clear antibacterial activity against Staphylococcus aureus. Additionally, the polymers were tested in terms of biocompatibility using the MTT viability assay. Here, some polymers were rated as cytotoxic while others showed good biocompatibility. Overall, polymers **A** and **N** have qualified for further experiments on titan plates in vitro as well as possible future investigations in a small animal model because notably, **N** showed intrinsic antibacterial properties, and both polymers have shown biocompatibility as well as very good anti-adhesive properties for both fibroblasts and tenocytes.

All in all, one should always take into consideration, that these results were obtained with in vitro cultures and a translatability to conclusions in vivo cannot easily be drawn. This, however, represents an extremely promising and novel approach in the development of anti-adhesive and yet anti-microbial acting polymer coatings for short-term implants and further investigations for their potential use in vivo will be needed to be able to reduce implant-associated complications in the future.

Literature

1. Ishiyama N, Moro T, Ishihara K, Ohe T, Miura T, Konno T, et al. The prevention of peritendinous adhesions by a phospholipid polymer hydrogel formed in situ by spontaneous intermolecular interactions. Biomaterials. 2010;31(14):4009-16.
2. Krettek C, Müller C, Meller R, Jagodzinski M, Hildebrand F, Gaulke R. [Is routine implant removal after trauma surgery sensible?]. Unfallchirurg. 2012;115(4):315-22.
3. Heinz T, Eidmann A, Jakuscheit A, Laux T, Rudert M, Stratos I. Demographics and Trends for Inbound Medical Tourism in Germany for Orthopedic Patients before and during the COVID-19 Pandemic. International Journal of Environmental Research and Public Health. 2023;20(2):1209.
4. Acklin YP, Bircher A, Morgenstern M, Richards RG, Sommer C. Benefits of hardware removal after plating. Injury. 2018;49:S91-S5.
5. Ip WY, Ng KH, Chow SP. A prospective study of 924 digital fractures of the hand. Injury. 1996;27(4):279-85.
6. Nichols AEC, Best KT, Loiselle AE. The cellular basis of fibrotic tendon healing: challenges and opportunities. Transl Res. 2019;209:156-68.
7. Scholes S, Panesar S, Shelton NJ, Francis RM, Mirza S, Mindell JS, Donaldson LJ. Epidemiology of lifetime fracture prevalence in England: a population study of adults aged 55 years and over. Age and Ageing. 2013;43(2):234-40.
8. Court-Brown CM, McQueen MM. Global Forum: Fractures in the Elderly. JBJS. 2016;98(9):e36.
9. Rupp M, Walter N, Pfeifer C, Lang S, Kerschbaum M, Krutsch W, et al. The Incidence of Fractures Among the Adult Population of Germany–an Analysis From 2009 through 2019. Dtsch Arztebl Int. 2021;118(40):665-9.
10. Siemers F. Konservative und operative Therapie von Mittelhandfrakturen. Trauma und Berufskrankheit. 2016;18(4):366-71.
11. Einhorn TA, Gerstenfeld LC. Fracture healing: mechanisms and interventions. Nat Rev Rheumatol. 2015;11(1):45-54.
12. Yamagiwa H, Endo N. [Bone fracture and the healing mechanisms. Histological aspect of fracture healing. Primary and secondary healing]. Clin Calcium. 2009;19(5):627-33.
13. Marsell R, Einhorn TA. The biology of fracture healing. Injury. 2011;42(6):551-5.
14. Rausch V, Seybold D, Königshausen M, Köller M, Schildhauer T, Geßmann J. Grundlagen der Knochenbruchheilung. Der Orthopäde. 2017;46(8):640-7.
15. Badia JM, Casey AL, Petrosillo N, Hudson PM, Mitchell SA, Crosby C. Impact of surgical site infection on healthcare costs and patient outcomes: a systematic review in six European countries. Journal of Hospital Infection. 2017;96(1):1-15.
16. Horan TC, Andrus M, Dudeck MA. CDC/NHSN surveillance definition of health care–associated infection and criteria for specific types of infections in the acute care setting. American Journal of Infection Control. 2008;36(5):309-32.
17. Zou X, Li X, He K, Song Q, Yin R. Current knowledge of vertebral osteomyelitis: a review. Eur J Clin Microbiol Infect Dis. 2025;44(2):213-31.
18. Wloch C, Wilson J, Lamagni T, Harrington P, Charlett A, Sheridan E. Risk factors for surgical site infection following caesarean section in England: results from a multicentre cohort study. BJOG: An International Journal of Obstetrics & Gynaecology. 2012;119(11):1324-33.
19. Gorvetzian JW, Epler KE, Schrader S, Romero JM, Schrader R, Greenbaum A, McKee R. Operating room staff and surgeon documentation curriculum improves wound classification accuracy. Heliyon. 2018;4(8):e00728.
20. Cheadle WG. Risk factors for surgical site infection. Surg Infect (Larchmt). 2006;7 Suppl 1:S7-11.
21. Pochhammer J, Harnoss JC, Walger P, Heidecke CD, Maier S, Kramer A. Vermeidung postoperativer Wundinfektionen. Allgemein- und Viszeralchirurgie up2date. 2016;10(04):241-57.
22. Sartelli M, Guirao X, Hardcastle TC, Kluger Y, Boermeester MA, Raşa K, et al. 2018 WSES/SIS-E consensus conference: recommendations for the management of skin and soft-tissue infections. World Journal of Emergency Surgery. 2018;13(1):58.

23. Lew DP, Waldvogel FA. Osteomyelitis. The Lancet. 2004;364(9431):369-79.
24. Walter G, Kemmerer M, Kappler C, Hoffmann R. Treatment algorithms for chronic osteomyelitis. Dtsch Arztebl Int. 2012;109(14):257-64.
25. Militz M, Ellenrieder M. Management bei Verdacht auf frühe Infektion nach Osteosynthese. Der Chirurg. 2021;92(10):963-72.
26. Stewart PS. Mechanisms of antibiotic resistance in bacterial biofilms. Int J Med Microbiol. 2002;292(2):107-13.
27. Bury DC, Rogers TS, Dickman MM. Osteomyelitis: Diagnosis and Treatment. Am Fam Physician. 2021;104(4):395-402.
28. Wang X, Zhang M, Zhu T, Wei Q, Liu G, Ding J. Flourishing Antibacterial Strategies for Osteomyelitis Therapy. Adv Sci (Weinh). 2023;10(11):e2206154.
29. Calhoun JH, Manring MM, Shirtliff M. Osteomyelitis of the long bones. Semin Plast Surg. 2009;23(2):59-72.
30. Hellebrekers P, Leenen LPH, Hoekstra M, Hietbrink F. Effect of a standardized treatment regime for infection after osteosynthesis. Journal of Orthopaedic Surgery and Research. 2017;12(1):41.
31. Evans JT, Evans JP, Walker RW, Blom AW, Whitehouse MR, Sayers A. How long does a hip replacement last? A systematic review and meta-analysis of case series and national registry reports with more than 15 years of follow-up. Lancet. 2019;393(10172):647-54.
32. Wu W, Cheng R, das Neves J, Tang J, Xiao J, Ni Q, et al. Advances in biomaterials for preventing tissue adhesion. J Control Release. 2017;261:318-36.
33. Liao J, Li X, Fan Y. Prevention strategies of postoperative adhesion in soft tissues by applying biomaterials: Based on the mechanisms of occurrence and development of adhesions. Bioact Mater. 2023;26:387-412.
34. Robertson D, Lefebvre G, Leyland N, Wolfman W, Allaire C, Awadalla A, et al. Adhesion prevention in gynaecological surgery: no. 243, June 2010. International Journal of Gynecology & Obstetrics. 2010;111(2):193-7.
35. Foster DS, Marshall CD, Gulati GS, Chinta MS, Nguyen A, Salhotra A, et al. Elucidating the fundamental fibrotic processes driving abdominal adhesion formation. Nat Commun. 2020;11(1):4061.
36. Chen J, Tang X, Wang Z, Perez A, Yao B, Huang K, et al. Techniques for navigating postsurgical adhesions: Insights into mechanisms and future directions. Bioeng Transl Med. 2023;8(6):e10565.
37. Barber CC, Burnham M, Ojameruaye O, McKee MD. A systematic review of the use of titanium versus stainless steel implants for fracture fixation. OTA Int. 2021;4(3):e138.
38. Sinicropi SM, Su BW, Raia FJ, Parisien M, Strauch RJ, Rosenwasser MP. The effects of implant composition on extensor tenosynovitis in a canine distal radius fracture model. The Journal of hand surgery. 2005;30(2):300-7.
39. Pillukat T, Windolf J, van Schoonhoven J. [Tenoarthrolysis after flexor tendon injuries]. Unfallchirurg. 2020;123(2):104-13.
40. Hohendorff B, Kaya H, Spies CK, Unglaub F, Müller LP, Ries C. [Tenolysis of extensor and flexor tendons of the hand]. Orthopade. 2020;49(9):771-83.
41. Borcherding K, Schmidmaier G, Hofmann GO, Wildemann B. The rationale behind implant coatings to promote osteointegration, bone healing or regeneration. Injury. 2021;52:S106-S11.
42. Satchanska G, Davidova S, Petrov PD. Natural and Synthetic Polymers for Biomedical and Environmental Applications. Polymers (Basel). 2024;16(8).
43. Oleksy M, Dynarowicz K, Aebisher D. Advances in Biodegradable Polymers and Biomaterials for Medical Applications-A Review. Molecules. 2023;28(17).
44. Asahara H, Inui M, Lotz MK. Tendons and Ligaments: Connecting Developmental Biology to Musculoskeletal Disease Pathogenesis. J Bone Miner Res. 2017;32(9):1773-82.
45. Bi Y, Ehirchiou D, Kilts TM, Inkson CA, Embree MC, Sonoyama W, et al. Identification of tendon stem/progenitor cells and the role of the extracellular matrix in their niche. Nature Medicine. 2007;13(10):1219-27.
46. Connizzo BK, Yannascoli SM, Soslowsky LJ. Structure-function relationships of postnatal tendon development: a parallel to healing. Matrix Biol. 2013;32(2):106-16.

47. Zschäbitz A. Anatomie und Verhalten von Sehnen und Bändern. Der Orthopäde. 2005;34(6):516-25.
48. Benjamin M, Kumai T, Milz S, Boszczyk BM, Boszczyk AA, Ralphs JR. The skeletal attachment of tendons--tendon "entheses". Comp Biochem Physiol A Mol Integr Physiol. 2002;133(4):931-45.
49. Wang JH, Guo Q, Li B. Tendon biomechanics and mechanobiology--a minireview of basic concepts and recent advancements. J Hand Ther. 2012;25(2):133-40; quiz 41.
50. Chen X, Yin Z, Chen JL, Shen WL, Liu HH, Tang QM, et al. Force and scleraxis synergistically promote the commitment of human ES cells derived MSCs to tenocytes. Sci Rep. 2012;2:977.
51. Bobzin L, Roberts RR, Chen HJ, Crump JG, Merrill AE. Development and maintenance of tendons and ligaments. Development. 2021;148(8).
52. Milz S, Ockert B, Putz R. Tenozyten und extrazelluläre Matrix. Der Orthopäde. 2009;38(11):1071-9.
53. Shukunami C, Takimoto A, Oro M, Hiraki Y. Scleraxis positively regulates the expression of tenomodulin, a differentiation marker of tenocytes. Dev Biol. 2006;298(1):234-47.
54. Docheva D, Hunziker EB, Fässler R, Brandau O. Tenomodulin is necessary for tenocyte proliferation and tendon maturation. Mol Cell Biol. 2005;25(2):699-705.
55. Chiquet-Ehrismann R, Tucker RP. Connective tissues: signalling by tenascins. Int J Biochem Cell Biol. 2004;36(6):1085-9.
56. Dilorio SE, Young B, Parker JB, Griffin MF, Longaker MT. Understanding Tendon Fibroblast Biology and Heterogeneity. Biomedicines. 2024;12(4).
57. Thomopoulos S, Parks WC, Rifkin DB, Derwin KA. Mechanisms of tendon injury and repair. J Orthop Res. 2015;33(6):832-9.
58. Kaya M, Karahan N, Yılmaz B. Tendon structure and classification. Tendons: IntechOpen; 2019. p. 1-9.
59. Lomas AJ, Ryan CN, Sorushanova A, Shologu N, Sideri AI, Tsioli V, et al. The past, present and future in scaffold-based tendon treatments. Adv Drug Deliv Rev. 2015;84:257-77.
60. Zhang Q, Yang Y, Yildirimer L, Xu T, Zhao X. Advanced technology-driven therapeutic interventions for prevention of tendon adhesion: Design, intrinsic and extrinsic factor considerations. Acta Biomater. 2021;124:15-32.
61. Wong JK, Lui YH, Kapacee Z, Kadler KE, Ferguson MW, McGrouther DA. The cellular biology of flexor tendon adhesion formation: an old problem in a new paradigm. Am J Pathol. 2009;175(5):1938-51.
62. Zhao X, Jiang S, Liu S, Chen S, Lin ZY, Pan G, et al. Optimization of intrinsic and extrinsic tendon healing through controllable water-soluble mitomycin-C release from electrospun fibers by mediating adhesion-related gene expression. Biomaterials. 2015;61:61-74.
63. Muhl L, Genové G, Leptidis S, Liu J, He L, Mocci G, et al. Single-cell analysis uncovers fibroblast heterogeneity and criteria for fibroblast and mural cell identification and discrimination. Nat Commun. 2020;11(1):3953.
64. Talbott HE, Mascharak S, Griffin M, Wan DC, Longaker MT. Wound healing, fibroblast heterogeneity, and fibrosis. Cell Stem Cell. 2022;29(8):1161-80.
65. Best KT, Korcari A, Mora KE, Nichols AE, Muscat SN, Knapp E, et al. Scleraxis-lineage cell depletion improves tendon healing and disrupts adult tendon homeostasis. Elife. 2021;10.
66. De Micheli AJ, Swanson JB, Disser NP, Martinez LM, Walker NR, Oliver DJ, et al. Single-cell transcriptomic analysis identifies extensive heterogeneity in the cellular composition of mouse Achilles tendons. Am J Physiol Cell Physiol. 2020;319(5):C885-c94.
67. Kendal AR, Layton T, Al-Mossawi H, Appleton L, Dakin S, Brown R, et al. Multi-omic single cell analysis resolves novel stromal cell populations in healthy and diseased human tendon. Sci Rep. 2020;10(1):13939.
68. Still C, 2nd, Chang WT, Sherman SL, Sochacki KR, Dragoo JL, Qi LS. Single-cell transcriptomic profiling reveals distinct mechanical responses between normal and diseased tendon progenitor cells. Cell Rep Med. 2021;2(7):100343.

69. Guo J, Tang H, Huang P, Ye X, Tang C, Shu Z, et al. Integrative single-cell RNA and ATAC sequencing reveals that the FOXO1-PRDX2-TNF axis regulates tendinopathy. Front Immunol. 2023;14:1092778.
70. Harvey T, Flamenco S, Fan CM. A Tppp3(+)Pdgfra(+) tendon stem cell population contributes to regeneration and reveals a shared role for PDGF signalling in regeneration and fibrosis. Nat Cell Biol. 2019;21(12):1490-503.
71. Titan AL, Foster DS, Chang J, Longaker MT. Flexor Tendon: Development, Healing, Adhesion Formation, and Contributing Growth Factors. Plast Reconstr Surg. 2019;144(4):639e-47e.
72. Carmont MR, Knutsson SB, Brorsson A, Karlsson J, Nilsson-Helander K. The release of adhesions improves outcome following minimally invasive repair of Achilles tendon rupture. Knee Surg Sports Traumatol Arthrosc. 2022;30(3):1109-17.
73. Zhang J, Wang JH. The effects of mechanical loading on tendons--an in vivo and in vitro model study. PLoS One. 2013;8(8):e71740.
74. Woo SL, Gelberman RH, Cobb NG, Amiel D, Lothringer K, Akeson WH. The importance of controlled passive mobilization on flexor tendon healing. A biomechanical study. Acta Orthop Scand. 1981;52(6):615-22.
75. Dick MK, Miao JH, Limaiem F. Histology, Fibroblast. StatPearls. Treasure Island (FL): StatPearls Publishing

Copyright © 2024, StatPearls Publishing LLC.; 2024.
76. Sigma-Aldrich. Data Sheet Accutase Solution [Available from: https://www.sigmaaldrich.com/specification-sheets/330/436/A6964-100ML-PW.pdf.
77. Tsien RY. THE GREEN FLUORESCENT PROTEIN. Annual Review of Biochemistry. 1998;67(Volume 67, 1998):509-44.
78. Leinweber B, Tang JX, Stafford WF, Chalovich JM. Calponin Interaction with α-Actinin-Actin: Evidence for a Structural Role for Calponin. Biophysical Journal. 1999;77(6):3208-17.
79. Haktaniyan M, Bradley M. Polymers showing intrinsic antimicrobial activity. Chemical Society Reviews. 2022;51(20):8584-611.
80. Zhang E, Song B, Shi Y, Zhu H, Han X, Du H, et al. Fouling-resistant zwitterionic polymers for complete prevention of postoperative adhesion. Proceedings of the National Academy of Sciences. 2020;117(50):32046-55.
81. Mayes SM, Davis J, Scott J, Aguilar V, Zawko SA, Swinnea S, et al. Polysaccharide-based films for the prevention of unwanted postoperative adhesions at biological interfaces. Acta Biomater. 2020;106:92-101.
82. Meier Bürgisser G, Calcagni M, Müller A, Bonavoglia E, Fessel G, Snedeker JG, et al. Prevention of peritendinous adhesions using an electrospun DegraPol polymer tube: a histological, ultrasonographic, and biomechanical study in rabbits. Biomed Res Int. 2014;2014:656240.
83. Böker KO, Gätjen L, Dölle C, Vasic K, Taheri S, Lehmann W, Schilling AF. Reduced Cell Adhesion on LightPLAS-Coated Implant Surfaces in a Three-Dimensional Bioreactor System. Int J Mol Sci. 2023;24(14).
84. Kuhn S, Kroth J, Ritz U, Hofmann A, Brendel C, Müller LP, et al. Reduced fibroblast adhesion and proliferation on plasma-modified titanium surfaces. J Mater Sci Mater Med. 2014;25(11):2549-60.
85. Präbst K, Engelhardt H, Ringgeler S, Hübner H. Basic Colorimetric Proliferation Assays: MTT, WST, and Resazurin. Methods Mol Biol. 2017;1601:1-17.
86. Mosmann T. Rapid colorimetric assay for cellular growth and survival: application to proliferation and cytotoxicity assays. Journal of immunological methods. 1983;65(1-2):55-63.
87. Markossian S GA, Baskir H, et al. . Assay Guidance Manual Eli Lilly & Company and the National Center for Advancing Translational Sciences 2013 [cited 2025 08.09.2025].
88. Ghasemi M, Turnbull T, Sebastian S, Kempson I. The MTT Assay: Utility, Limitations, Pitfalls, and Interpretation in Bulk and Single-Cell Analysis. International Journal of Molecular Sciences. 2021;22(23):12827.

89. Wagenhäuser MU, Pietschmann MF, Sievers B, Docheva D, Schieker M, Jansson V, Müller PE. Collagen type I and decorin expression in tenocytes depend on the cell isolation method. BMC Musculoskelet Disord. 2012;13:140.
90. Han SH, Kim HK, Ahn JH, Lee DH, Baek M, Ye G, et al. A Protocol to Acquire the Degenerative Tenocyte from Humans. J Vis Exp. 2018(136).
91. Magill SS, Edwards JR, Bamberg W, Beldavs ZG, Dumyati G, Kainer MA, et al. Multistate point-prevalence survey of health care-associated infections. N Engl J Med. 2014;370(13):1198-208.
92. Anderson JM. Future challenges in the in vitro and in vivo evaluation of biomaterial biocompatibility. Regen Biomater. 2016;3(2):73-7.
93. Arciola CR, Campoccia D, Speziale P, Montanaro L, Costerton JW. Biofilm formation in Staphylococcus implant infections. A review of molecular mechanisms and implications for biofilm-resistant materials. Biomaterials. 2012;33(26):5967-82.
94. Chen X, Zhou J, Qian Y, Zhao L. Antibacterial coatings on orthopedic implants. Mater Today Bio. 2023;19:100586.
95. Cloutier M, Mantovani D, Rosei F. Antibacterial Coatings: Challenges, Perspectives, and Opportunities. Trends Biotechnol. 2015;33(11):637-52.
96. Banerjee I, Pangule RC, Kane RS. Antifouling coatings: recent developments in the design of surfaces that prevent fouling by proteins, bacteria, and marine organisms. Adv Mater. 2011;23(6):690-718.
97. Chen T, Zhao L, Wang Z, Zhao J, Li Y, Long H, et al. Hierarchical Surface Inspired by Geminized Cationic Amphiphilic Polymer Brushes for Super-Antibacterial and Self-Cleaning Properties. Biomacromolecules. 2020;21(12):5213-21.
98. Xu LC, Li Z, Tian Z, Chen C, Allcock HR, Siedlecki CA. A new textured polyphosphazene biomaterial with improved blood coagulation and microbial infection responses. Acta Biomater. 2018;67:87-98.
99. Darmanin T, Guittard F. Recent advances in the potential applications of bioinspired superhydrophobic materials. Journal of Materials Chemistry A. 2014;2(39):16319-59.
100. Cloutier M, Mantovani D, Rosei F. Antibacterial Coatings: Challenges, Perspectives, and Opportunities. Trends in Biotechnology. 2015;33(11):637-52.
101. Martínez-Moreno J, Merino V, Nácher A, Rodrigo JL, Climente M, Merino-Sanjuán M. Antibiotic-loaded Bone Cement as Prophylaxis in Total Joint Replacement. Orthop Surg. 2017;9(4):331-41.
102. Sanderson PL, Ryan W, Turner PG. Complications of metalwork removal. Injury. 1992;23(1):29-30.
103. Rezaei AR, Zienkiewicz D, Rezaei AR. Surgical site infections: a comprehensive review. J Trauma Inj. 2025;38(2):71-81.

8 Attachments

Parts of this work have been previously published in scientific publications.

Wiesner F, Schönewald KGM, **Vogel K**, Jung N, Schwierz B, Kipping M, Ibragimova A, Schumacher J, Pritzel C, Thiagarajan CRV, Ritz U, Jonas U. Antiadhesive and Antibacterial Coatings for Short-Term Titanium Implants. Macromol Rapid Commun. 2025 Jun;46(12):e2400989. doi: 10.1002/marc.202400989. Epub 2025 Mar 8. PMID: 40056084; PMCID: PMC12183145.

An application has been filed for the following patent:

Patent: WO2024094645A1-“Nonstick polymer coatings for short-term implants”, Inventors: Niklas Jung, Ulrich Jonas, Fiona Wiesner (née Diehl), Clinton Richard Viktor Thiagarajan, Ulrike Ritz, Karl Michael Georg Schönewald, **Kira Vogel**

9 Acknowledgements

10 Curriculum vitae